We are IntechOpen, the world's leading publisher of Open Access books Built by scientists, for scientists

4,800
Open access books available

122,000
International authors and editors

135M
Downloads

Our authors are among the

154
Countries delivered to

TOP 1%
most cited scientists

12.2%
Contributors from top 500 universities

CLARIVATE ANALYTICS BOOK CITATION INDEX INDEXED

WEB OF SCIENCE™

Selection of our books indexed in the Book Citation Index in Web of Science™ Core Collection (BKCI)

Interested in publishing with us?
Contact book.department@intechopen.com

Numbers displayed above are based on latest data collected.
For more information visit www.intechopen.com

3

Frequency-Domain Objective Response Detection Techniques Applied to Evoked Potentials: A Review

Danilo Barbosa Melges[1,2], Antonio Mauricio Ferreira Leite Miranda de Sá[1] and Antonio Fernando Catelli Infantosi[1]

[1]*Biomedical Engineering Program, Federal University of Rio de Janeiro (UFRJ)*
[2]*Electrical Engineering Department, Federal University of Minas Gerais (UFMG)*
Brazil

1. Introduction

The Electroencephalogram (EEG) is the biological signal collected at the scalp as a summation result of ionic currents generated from the post-synaptic potentials of the brain neurons. Differently from some other biosignals such as the electrocardiogram, which presents a visual identifiable pattern – particularly the QRS complex, the EEG exhibits a very large random variability. It is indeed quite often assumed to be a white Gaussian noise, and this stochastic behavior turns the analysis of EEG signals by visual inspection a very difficult task. In spite of this, the EEG is known to be correlated with sensorial information processing, and it is widely used for neurophysiologic assessment and neuropathies diagnosis.

The cortical response obtained by sensorial excitation consists of a neurological evaluation paradigm that produces a pattern related to a stimulation that is often rhythmic, such as electric pulses, auditory clicks or intermittent light. The elicited cortical activity is usually synchronized with the stimulation, but it is embedded in the spontaneous EEG, which has much higher amplitude values. An estimation of this evoked response is frequently obtained by averaging EEG epochs stimuli-synchronized. The resulting waveform is visually inspected and evaluated by a neurologist or a technical specialist for both diagnosis/prognosis and surgical monitoring purposes. Such response is locked in time and phase with the stimulation, which can lead to a clear pattern that is usually called evoked potential (EP).

The most employed evoked potentials are the visual (VEP) – elicited by intermittent photic stimuli-, the auditory (AEP) – obtained by tones or clicks-, and the somatosensory ones (SEP), evoked by electric current pulses. Among many applications, the VEP is commonly applied for visual acuity evaluation of infants and newborns (Linden *et al.*, 1997); the AEP is often used for monitoring the depth of anesthesia (Cagy, 2003) and auditory screening of newborns (Ramos *et al.*, 2000); whilst the SEP is frequently employed for monitoring spine (Cruccu *et al.*, 2008) and vascular surgeries (Keyhani *et al.*, 2009).

Although the EP has been widely applied, the conventional procedure is based on the physician experience and ability, as well as in informal criteria (Dobie and Wilson, 1993). The analysis is also hampered by the EEG recording quality, anesthesia regimen, and the high variability inter-observer and inter-patient (Martin *et al.*, 2002). In order to overcome these limitations and aiming at widening the employment of the evoked potentials, the use of Objective Response Detection (ORD) techniques has been proposed. One of the first works applying the ORD to evoked potentials was described in Galambos *et al.* (1984 apud Stapells *et al.*, 1987), which introduced the Phase Coherence. Since then, many other ORD techniques have been investigated.

These methods are based on statistical tests that allow inferring about the presence (or absence) of sensory response with a maximum false-positive rate previously established, which is the significance level of the statistical test. The ORD techniques at the frequency domain are useful, particularly in the presence of narrow band noises, such as network noise and its harmonics. This kind of noise corrupts the EP waveform, yielding to a misleading analysis and, consequently, to a mistaken diagnose or monitoring. However, it only affects the frequency-domain ORD in specific frequencies that can be disregarded in the analysis. Hence, these techniques are more suitable for medical environments (hospitals and intensive care units), which are usually electrically noisy, due to the presence of many electrical and electro-mechanical devices.

Although the ORD allows reducing the subjectivity of neurophysiologic assessment, the probability and rapidness of detection are still aspects to be optimized. The fast detection with high hit rate is a requirement specially for intra-operative monitoring, since it can help the physicians to avoid iatrogenic neurological damages. Methods to accelerate the detection such as the application of a decreasing exponential (Tierra-Criollo *et al.*, 1998) to the ORD techniques have been proposed. More recently, the employment of more than one EEG derivation in a multivariate ORD approach has been suggested in order to improve the detection probability (Miranda de Sá and Felix, 2002). These techniques constitute the state of the art for objectively identify sensorial responses to a stimulation.

This work aims at reviewing the most employed frequency-domain techniques applied to evoked potentials. Besides the Introduction, this chapter will be subdivided into six sections. The second one introduces the model of evoked response generation. Section 3 presents a brief description of the principal applications of the cortical (brain) responses obtained by different types of stimulation (visual, auditory and somatosensory). Both clinical diagnosis and surgical monitoring references are included. In the next section, the mathematical definition of uni- and multivariate techniques is provided. A chronological literature review of applying the ORD to EP is described in Section 5. The subsequent section presents examples of using these techniques, including recent findings. Finally, the last section discloses a discussion about ORD.

2. The model of evoked potential generation and the coherent average

The evoked potential (EP) generation model is shown in Figure 1, where $v[k]$ is the response elicited by the sensory stimulation $x[k]$, $b[k]$ is the spontaneous EEG and $H(f)$ is the transfer function of the sensory pathways. The evoked response v[k] is considered to be identical from stimulus-to-stimulus (i.e. $H(f)$ is assumed to be deterministic) and the

background EEG is assumed to be a zero-mean white Gaussian noise. Hence, the measured EEG $y[k]$ is composed by evoked and background activities. In this linear model, a correlation between stimulus and EEG is expected at the stimulation frequency and its multiples.

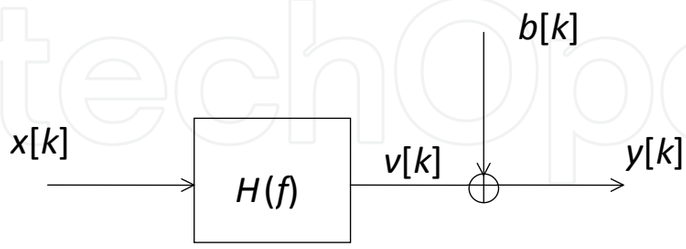

Fig. 1. Linear Model of evoked potential generation: $x[k]$ is the stimulus, $H(f)$ is the frequency-domain transfer function of the sensory pathways, $v[k]$ is the stimuli-response, $b[k]$ is the background EEG and $y[k]$ is the measured EEG.

This model reflects the scalp electrical activity registration, where the evoked potentials are usually embedded in the spontaneous (or background) EEG. Since the EP is tens of times lower than the background EEG, it cannot be visualized; therefore, it is common to perform the averaging of many epochs, taken the stimulus instant as the fiducial point. As mentioned above, assuming that the background EEG is a zero-mean Gaussian noise and the responses are synchronized with the stimulation and identical from stimulus to stimulus (Lopes da Silva, 1999), this procedure, known as coherent average, leads to an increase in the signal-to-noise ratio as shown next.

Considering the linear model presented in Figure 1, the i^{th} EEG epoch during stimulation can be given by:

$$y_i[k] = v[k] + n_i[k]$$

where $v[k]$ is the evoked response and $n[k]$ is the background EEG. The coherent average provides an estimate of the evoked potential, being calculated by:

$$\hat{v}[k] = \frac{1}{M}\sum_{i=1}^{M} y_i[k] = \frac{1}{M}\sum_{i=1}^{M} v[k] + \frac{1}{M}\sum_{i=1}^{M} n_i[k]$$

where the superscript ^ denotes estimation and M is the number of EEG epochs. When M tends to infinity, $\hat{v}[k]$ tends to $v[k]$, since the parcel due to summation involving the $n_i[k]$ terms will vanish.

3. Clinical and surgical application of the evoked potentials

The evoked potentials obtained by different kinds of stimulation have been applied to a broad range of clinical and intra-operative conditions. It is increasing the number of studies that shows the advantages of EP application for supporting the diagnosis of neuropathies and the continuous neuromonitoring in order to avoid neurological damages.

The Brainstem Auditory Evoked Potential (BAEP), elicited by click (sound pulses), is an important tool in the child auditory screening (Ramos *et al.*, 2000, Infantosi *et al.*, 2004), since it can assess the auditory pathways down to the brainstem. It is usually performed by obtaining the auditory neurophysiologic threshold by means of the BERA (Brainstem Evoked Response Audiometry). The most widely employed screening method is the optoacoustic emission (OE). Although this latter has been applied in many hospital units, due to its technical and operational facility (Zaeyen, 2005), the OE evaluate the integrity only up to the cochlea, whereas the BAEP can access the auditory pathways up to the brainstem. Moreover, there are cases in which the BAEP is absent or impaired, but the OE are preserved (Infantosi *et al.*, 2004). Thus, a question that naturally arises is whether the OE is a suitable method for auditory screening in newborn intensive care units (Infantosi *et al.*, 2004).

On the other hand, the BAEP has been also employed for intra-operative monitoring during removal of cerebello-pontine tumors, microvascular decompression of cranial nerves and ischemic complications due the manipulation of the posterior fossa circulation, since this potential is stable to a variety of anesthetics and pharmacological agents and presents adequate reproducibility (Linden *et al.*, 1997).

When the impairment is located in structures above the brainstem, the investigation of late potentials such as the Middle Latency Auditory Evoked Potential (MLAEP) can be suitable for functional evaluation up to the primary auditory cortex (Zaeyen, 2005). The MLAEP has been also applied for monitoring the depth anesthetic plan (Nayak and Roy, 1998, Gemal, 1999, Cagy and Infantosi, 2002, Cagy, 2003), because it presents changes that are dose-dependent with the anesthesia. The anesthetic plan monitoring is particularly important because the clinical signs usually applied for this purpose are masked by the employment of vasodilators, vasoconstrictors, calcium channel blockers and neuromuscular blockers during surgeries (Nayak and Roy, 1998).

The application of the Visual Evoked Potential (VEP) for monitoring is limited due to the need of controlling parameters such as surgical room light and distance between the eye and the stimulator. Although it has been used during surgeries of pituitary tumors and brain aneurisms, the recording of VEP for intra-operative functional evaluation presents low success rate (Linden et al., 1997). Flash-VEP is one of the potentials with the highest signal-to-noise ratio (SNR) , some characteristics of its waveform can be even visually identified with only 100 stimuli. Nevertheless, this potential shows high inter- and intra-observer variability, which makes difficult its evaluation with the administration of anesthetics. Moreover, since the quantity of light is a function of the pupil size, agents causing mydriasis (pupil dilatation) should be applied when anesthetics are administered (Linden et al., 1997). On the other hand, the VEP has been used, especially in pediatrics, for evaluating the visual acuity, detecting amblyopia, and as a useful tool for prognosis of comatose patients, newborn asphyxia and cortical blindness (Linden et al., 1997). Other applications of VEP includes diagnosis of migraine in children and adolescents (Jancic-Stefanovic *et al.*, 2003), childhood optical glioma (Trisciuzzi *et al.*, 2004) and functional visual loss (Xu *et al.*, 2001). It has also been used in studies of dyslexia (Schulte-Körne *et al.*, 2004), periventricular leukomalacia (Kato *et al.*, 2005), retinitis pigmentosa (Holopigian *et al.*, 2005), macular degeneration (Nemoto *et al.*, 2002), schizophrenia (Krishnan *et al.*, 2005), glaucoma (Parisi *et al.*, 2001) and nystagmus (Hoffmann *et al.*, 2004).

The somatosensory evoked potential (SEP) is often obtained by applying electric current pulses and is useful for detecting peripheral nerve lesions, plexopathies and radiculopathies (Linden *et al.*, 1997), and for monitoring vascular and spine surgeries such as desobstruction of the carotid artery (Liu *et al.*, 2010), aortic aneurism repair (Keyhani *et al.*, 2009, Van Dongen *et al.*, 2001), aortic coarctation repair (Faberowski *et al.*, 1999), scoliosis correction procedures (Cruccu *et al.*, 2008) and lumbar pedicle screw placement for in situ posterior spinal fusion (Gundanna, 2003), due to its sensitivity to mechanical stress, hypotension and ischemia.

The neuromonitoring is considered important in the prevention of immediate and late paraplegia caused by medullary ischemia, since it is capable of detecting the "ischemic penumbra", status pathophysiologic present in the acute ischemia, when the neurons are not at functional state, but alive and recoverable by the application of appropriate procedures (Guérit and Dion, 2002).

Due to its sensitivity to temperature, the SEP has been used as optimal temperature identifier during surgeries that require profound hypothermia (Ghariani *et al.*, 1999), being considered as a secure and efficient method (Ghariani *et al.*, 2000). The hypothermia is employed in order to reduce the cerebral metabolism, during surgeries of ascending aorta and aortic arch repair, which require circulatory arrest (Ghariani *et al.*, 1998). This procedure allows the reduction of neurological sequels arising from hypoxia. On the other hand, excessively low temperatures can lead to iatrogenic complications, such as coagulation disorders, hemolysis, increased blood viscosity, among others (Ghariani *et al.*, 2000).

The need of monitoring upper and lower limbs during surgeries has been reported due to the occurrence of paraplegia by unpredicted intra-operative evaluation of only median nerve SEP (Ghariani et al., 1999). The advantages that the monitoring of the four limbs SEP can provide for a low cost, reducing the occurrence of transient and persistent neurological complications, has been also reported by Jones et al. (2004). In a survey conducted with members of the Scoliosis Research Society, Nuwer et al. (1995) reported that 88% of the north-American surgeons used the SEP in more than a half of the surgeries. According to Bose et al. (2004), the neurophysiologic monitoring during lumbar and thoracic surgery has become a routine procedure for years, but its employment during cervical surgeries is more recent and seems to be a sensitive method for detecting neurological insults caused by mechanical stress, surgical manipulation, hypotension and ischemia.

Since it is related with variations in the cerebral blood flow, the SEP presents identifiable changes associated with variation in the hemodynamics (Florence et al., 2004). Moreover, the SEP is not influenced by muscular blockers and present gradual changes with the increase of anesthetic concentration (Angel et al., 1999). Frequently registered over the somatosensory cortex, region vascularized by the carotid artery, the SEP is often used during the carotid endarterectomy (Florence et al., 2004), performed for the treatment of vascular obstructive disease and that presents potential risk of ischemia for the ipsilateral hemisphere during internal carotid artery occlusion (Linden et al., 1997). The absence of the cortical function and of the subcortical EP, in cases of cerebral hemorrhages, is a negative prognostic predictor, although its preservation does not present prognostic value (Guérit, 1999).

For monitoring intracranial aneurysms repair surgeries, the real time detection of cerebral ischemia can help the surgeon, for example, to determine the duration of the temporary vascular occlusion and the optimal systemic arterial pressure (Martin et al., 2002). The SEP and the cortical EEG are the techniques most frequently employed for this purpose in anterior circulation aneurysm surgeries (Martin et al., 2002).

Apart from the cited surgeries, the SEP monitoring was also successfully applied in many other surgical procedures, such as interventional neuroradiology, stereotaxic surgery of the brainstem, thalamus, cerebral cortex, thalamotomy, cortical localization, brachial plexus surgery and pelvic fracture surgery (Linden et. al, 1997). SEP also presents prognostic value in cases of intracranial hypertension (Giugno et al., 2003) and coma (Logi et al., 2003).

Even when post-operative squeals cannot be avoided by monitoring, the detection of neurophysiologic intra-operative changes can make the surgery staff aware of the risk and avoid the exacerbation of the damage (Bose et al., 2004). However, it is important selecting the patients for whom the EP monitoring can be useful, because if the patient does not present pre-operative EP, this technique is not suitable for intra-operative neuro-evaluation (Linden et al., 1997).

Finally, as the neuromonitoring represents only the current status of the patient, many studies point out the importance of the post-surgery SEP monitoring in order to detect late neurological complications (Guérit and Dion, 2002, Dong et al., 2002, Ghariani et al., 2000).

4. Frequency–domain Objective Response Detection (ORD) techniques

This section describes some of the most used frequency-domain Objective Response Detection (ORD) techniques, both in its univariate and multivariate versions. Details about *a priori* assumptions related to the signals are included.

4.1 Univariate ORD techniques

4.1.1 Phase Coherence

The Phase Coherence (PC) was introduced in the analysis of the evoked potentials by Galambos *et al.* (1984) and can be seen as a statistical measure of the phase variance. It can be mathematically defined by:

$$\hat{\theta}_c(f) = \sqrt{\left(\sum_{i=1}^{M}\sin\phi_i(f)\right)^2 + \left(\sum_{i=1}^{M}\cos\phi_i(f)\right)^2} \Big/ M \tag{1}$$

where $\phi_i(f)$ is the phase angle of the ith Fourier Transformed EEG epoch and M is the number of EEG epochs. This measure supposes that the presence of stimuli-response causes a phase aggregation of the Fourier Transformed EEG epochs in the complex plan. On the other hand, on the absence of response, the phase angle is assumed to be randomly distributed between 0 and 2π, and the probability of obtaining this phase angle configuration is accessed by the Rayleigh test (Mardia, 1972). This techniques only takes into account the phase of the Fourier Transform (FT) of EEG epochs.

4.1.2 Hotelling's T^2 test

According to Picton et al. (1987), the Hotelling T^2 Test (HT2) is the multivariate analogue of the Student's t test. If M samples of a uni-variate distribution is taken, one can estimate its mean $\bar{y}$ and standard deviation s. Based on this two parameters, it is possible to calculate the limits for the occurrence of the population mean:

$$\sqrt{M}\frac{\left|\bar{y}-y\right|}{s} \le t$$

where t are the limits taken from the two-tailed Student's t distribution with M-1 degrees of freedom.

For a bidimensional distribution, the confidence region for the mean vector is given by:

$$M\left(\bar{Y}(f)-Y(f)\right)^{H} S^{-1}\left(\bar{Y}(f)-Y(f)\right) \le \hat{T}^2(f) \tag{2}$$

where the superscript H and ^ denote Hermitian and estimation, respectively, S^{-1} is the inverse of the covariance matrix of the sample, Y(f) is the vector of the M Fourier Transformed EEG epochs and $\bar{Y}(f)$ the mean vector.

The statistics T^2 can be related to the Fisher's F distribution by (Picton et al., 1987):

$$\hat{T}^2_{crit}(f) = \frac{(M-1)2}{(M-2)} F_{crit,2,M-2,\alpha} \tag{3}$$

where M is the number of epochs used to calculate the T^2 estimate and $F_{crit,2,M-2,\alpha}$ is the critical value of the F-distribution with 2 and M-2 degrees of freedom at the significance level α.

Considering that the Fourier Transformed EEG epochs are bidimensional variables (complex variables with real and imaginary parts), the confidence region for the mean vector leads to an ellipse of confidence. When the ellipse encompasses the origin of the plan (0,0), which represents the response absence condition, one can assume that there is no response to the stimulation. On the other hand, if the origin is not included in the confidence region, the null hypothesis of response absence can be rejected, and one can assume the response detection.

4.1.3 Spectral F Test (SFT)

The Spectral F Test (SFT) is given by the ratio between the Power Spectrum Density (PSD) of the EEG during stimulation $y[k]$ and the background EEG $b[k]$ (Dobie and Wilson, 1996). For windowed EEG signals, the SFT can be estimated by the ratio of the Bartlett periodograms, as follows:

$$\hat{\phi}(f) = \frac{\frac{1}{M_y}\sum_{i=1}^{M_x}\left|Y_i(f)\right|^2}{\frac{1}{M_b}\sum_{i=1}^{M_y}\left|B_i(f)\right|^2} \tag{4}$$

where the superscript ^denotes estimation, $Y_i(f)$ and $B_i(f)$ are, respectively, the Discrete Fourier Transform (DFT) of the ith EEG epoch of $y[k]$ and $b[k]$, and M_y and M_b, are the number of EEG epochs during stimulation and at the resting condition (background EEG), respectively.

In the null hypothesis (H_0) of no stimulus response, the EEG during stimulation belongs to the same population as the background EEG; hence, both $y[k]$ and $b[k]$ are zero-mean Gaussian noise with equal variance. Hence, it can be shown that the distribution of the SFT can be related to the Fisher F-distribution by:

$$\frac{M_y}{M_b}\hat{\phi}(f) \sim F_{2M_y,2M_b} \tag{5}$$

Thus, the critical value for a given significance level α, M_y and M_b number of EEG epochs is expressed by:

$$\hat{\phi}_{crit}(f) = F_{crit2M_y,2M_b,\alpha} \tag{6}$$

where $F_{crit2M_y,2M_b,\alpha}$ is the critical value of the F-distribution with $2M_y$ and $2M_b$ degrees of freedom.

The above expression for critical values calculation is not valid for DC (direct current) and Nyquist frequency, since, in these frequencies, the Fourier Transform of EEG epoch leads to purely real values.

4.1.4 Magnitude-Squared Coherence (MSC)

The squared modulus of the coherence function (also called Magnitude-squared coherence, MSC), $\gamma_{yx}^2(f)$, corresponds to the parcel of the squared mean value of the measured EEG signal $y[k]$ caused by the stimulation $x[k]$ for a given frequency f (Bendat and Piersol, 2000), and is calculated by (Dobie and Wilson, 1989):

$$\gamma_{yx}^2(f) = \frac{\left|G_{yx}(f)\right|^2}{G_{yy}(f)G_{xx}(f)} \tag{7}$$

where $G_{yx}(f)$ is the cross-spectrum of $x[k]$ and $y[k]$ normalized by the auto-spectra, $G_{yy}(f)$ and $G_{xx}(f)$. It can be shown that the MSC (expression 7) is a real function that varies between 0 and 1.

The estimates of $\gamma_{yx}^2(f)$ for discrete-time, finite-duration and windowed signals can be calculated by (Bendat and Piersol, 2000):

$$\hat{\gamma}_{yx}^2(f) = \frac{\left|\sum_{i=1}^{M} Y_i(f)X_i^*(f)\right|^2}{\sum_{i=1}^{M}\left|Y_i(f)\right|^2\sum_{i=1}^{M}\left|X_i(f)\right|^2} \tag{8}$$

where "^" superscript denotes estimation, * is the complex conjugate, M is the number of epochs, and $Y_i(f)$ and $X_i(f)$ are the Discrete Fourier Transform (DFT) of the ith epoch of signals $y[k]$ and $x[k]$, respectively.

For the case of a periodic stimulation ($x[k]$), $X_i(f)$ is identical for all epochs and the MSC estimate depends only on the measured EEG $Y_i(f)$, since the contribution of the periodic signal to both the numerator and denominator cancels out (Dobie and Wilson, 1989):

$$\hat{\kappa}^2(f) = \frac{\left|\sum_{i=1}^{M} X(f)Y_i(f)\right|^2}{M\sum_{i=1}^{M}\left|X(f)Y_i(f)\right|^2} = \frac{X^2(f)\left|\sum_{i=1}^{M} Y_i(f)\right|^2}{M\,X^2(f)\sum_{i=1}^{M}\left|Y_i(f)\right|^2}$$

$$\hat{\kappa}^2(f) = \frac{\left|\sum_{i=1}^{M} Y_i(f)\right|^2}{M\sum_{i=1}^{M}\left|Y_i(f)\right|^2} \tag{9}$$

From expression 9, it can be seen that, when there is no response to stimulation, the numerator corresponds only to background EEG (assumed to be a zero-mean white Gaussian noise) and, therefore, $\hat{\kappa}^2(f)$ tends to zero. On the other hand, if a consistent response is present in all epochs ($Y_i(f) = Y(f)$, $\forall i$), $\hat{\kappa}^2(f)$ tends to the unity.

For the null hypothesis (H_0) of response absence ($\kappa^2(f) = 0$, where $\kappa^2(f)$ is the true value of the MSC), it can be shown that, for M independent epochs of $y[k]$ (zero-mean white Gaussian noise, by assumption), the MSC can be related to the F-distribution by the following expression (Simpson et al., 2000):

$$(M-1)\frac{\hat{\kappa}^2(f)}{(1-\hat{\kappa}^2(f))} \sim F_{2,2M-2} \tag{10}$$

Hence, based on the critical values of the F-distribution, one can calculate the critical values for the MSC estimates for a given significance level α (Simpson et al., 2000):

$$\hat{\kappa}^2_{crit,\alpha} = \frac{F_{crit2,2M-2,\alpha}}{M-1+F_{crit2,2M-2,\alpha}} \tag{11}$$

The critical value constitutes a detection threshold and can be alternatively calculated by the following analytical expression (Miranda de Sá and Infantosi, 2007):

$$\hat{\kappa}^2_{\text{crit}} = 1-\alpha^{\frac{1}{M-1}} \tag{12}$$

The detection is based on rejecting the null hypothesis (H_0) of response absence, which is reached when the estimate values exceed the critical value ($\hat{\kappa}^2(f) > \hat{\kappa}^2 crit$).

Considering the linear model presented in Section 2, the response detection is expected in the stimulation frequency and its harmonics. Even in the no-stimulation condition, the detection is expected at the rate of α, that is, the significance level of the statistical test corresponds to the maximum false positive rate. The above mentioned critical values are not valid for DC and Nyquist frequency, since the DFT of these components are purely real, while $Y_i(f)$ is complex for other frequencies.

4.1.5 Magnitude-Squared Coherence (MSC) with Exponential Forgetting (MSC-EF)

The application of an exponential forgetting to the MSC was proposed by Tierra-Criollo et al. (1998) and consists of the employment of a decreasing exponential to the EEG epochs spectra, as follows:

$$\hat{\kappa}_p^2(i,f) = (1-b)\frac{\left|Y_i(f) + bS'_{i-1}(f)\right|^2}{\left|Y_i(f)\right|^2 + bS''_{i-1}(f)} \tag{13}$$

being

$$S'_i(f) = Y_i(f) + bS'_{i-1}(f)$$

$$S''_i(f) = \left|Y_i(f)\right|^2 + bS''_{i-1}(f)$$

where *f* is the frequency index, ^ denotes estimation, $Y_i(f)$ represents the DFT of the ith EEG epoch and *b* is the forgetting factor (0<*b*<1).

According to Tierra-Criollo et al. (1998), for the null hypothesis of response absence (H_0), similarly to the described for the MSC, $\hat{\kappa}_p^2(f)$ can be related to the F-distribution:

$$(M'-1)\frac{\hat{\kappa}_p^2(f)}{(1-\hat{\kappa}_p^2(f))} \sim F_{2,2M'-2} \tag{14}$$

where $F_{2,2M'-2}$ is the F-distribution with *2* and *2M'-2* degrees of freedom and *M'* is given by:

$$M' = \frac{1+b}{1-b} \tag{15}$$

Thus, based on the critical values of $F_{2,2M'-2}$, one can obtain the critical values for $\hat{\kappa}_p^2(f)$ with a given significance level α:

$$\hat{\kappa}_{p_{crit}}^2 = \frac{F_{crit2,2M'-2,\alpha}}{M'-1+F_{crit2,2M'-2,\alpha}} \tag{16}$$

Similarly to the mentioned for MSC, the response detection ($\hat{\kappa}_p^2(f) > \hat{\kappa}_{p_{crit}}^2$) is expected at the stimulation frequencies and its harmonics. Even in the no-stimulation condition, the detection is expected at the rate of the significance level of the statistical test.

The critical value can be alternatively calculated by the following analytical expression:

$$\hat{\kappa}^2_{\text{crit}} = 1 - \alpha^{\frac{1}{M'-1}} \tag{17}$$

4.1.6 Component Synchrony Measure (CSM)

The Component Synchrony Measure (CSM) or Phase Synchrony Measure (PSM) quantifies the degree of synchronism between frequencies of a signal, taking into account only the phase of its Fourier Transform (Simpson et al., 2000):

$$\hat{\rho}^2(f) = \left[\frac{1}{M}\sum_{i=1}^{M}\cos\phi_i(f)\right]^2 + \left[\frac{1}{M}\sum_{i=1}^{M}\sin\phi_i(f)\right]^2 \tag{18}$$

where $\phi_i(f)$ is the phase of the Fourier Transform of the i^{th} EEG epoch and M is the number of epochs used in the CSM estimation.

Assuming that the phase is uniformly distributed between 0 and 2π (absence of synchronism between stimulus and response), the probability density function is given by $1/2\pi$ and the functions $\cos\phi_i$ and $\text{sen}\phi_i$ present zero mean and variance ½ (Miranda de Sá and Felix, 2003), as follows:

$$\mu = \int_0^{2\pi}\cos\phi\frac{1}{2\pi}d\phi = \int_0^{2\pi} sen\phi\frac{1}{2\pi}d\phi = 0$$

$$\sigma^2 = \int_0^{2\pi}\cos^2\phi\frac{1}{2\pi}d\phi = \int_0^{2\pi} sen^2\phi\frac{1}{2\pi}d\phi = \frac{1}{2}$$

According to the Central Limit Theorem, the summation of sins (and co-sins) in the expression 18 tends asymptotically to a normal distribution with zero-mean and variance M/2:

$$\sum_{i=1}^{M}\cos\phi_i \sim N\left(0,\frac{M}{2}\right) \quad and \quad \sum_{i=1}^{M} sen\phi_i \sim N\left(0,\frac{M}{2}\right)$$

Hence, it can be shown that:

$$\frac{\left(\sum_{i=1}^{M}\cos\phi_i\right)^2 + \left(\sum_{i=1}^{M} sen\phi_i\right)^2}{M/2} \sim \chi^2_2$$

where χ^2_2 is the chi-squared distribution with 2 degrees of freedom. From this expression, the CSM can be related to the χ^2_2 distribution by:

$$\hat{\rho}^2(f) \sim \frac{1}{M^2}\frac{M}{2}\chi_2^2 = \frac{\chi_2^2}{2M} \tag{19}$$

Thus, for the null hypothesis of absence of synchronism, the critical value for a given significance level α and *M* EEG epochs can be obtained by (Mardia, 1972):

$$\rho_{crit,\alpha}^2 = \frac{\chi_{2\,crit,\alpha}^2}{2M} \tag{20}$$

where $\chi_{2\,crit,\alpha}^2$ is the critical value of the chi-squared distribution for the significance level α. It is worth noting that CSM expression corresponds to the square of the Phase Coherence (PC).

Alternatively, the critical value for CSM can be calculated based on the probability density function of the chi-squared distribution given as:

$$p_{\chi_2^2}(z) = \frac{1}{2}e^{-\frac{z}{2}}.$$

The analytical critical value of χ_2^2 for a given significance level α is obtained from

$$\int_0^{\chi_{2crit}^2} \frac{1}{2}e^{-\frac{z}{2}}dz = 1-\alpha,$$

which yields to:

$$\chi_{2\,crit,\alpha}^2 = 2\ln\left(\frac{1}{\alpha}\right). \tag{21}$$

Hence, substituting expression (21) in (20) leads to:

$$\rho_{crit,\alpha}^2 = \frac{\ln(1/\alpha)}{M} \tag{22}$$

4.2 Multivariate ORD (MORD) techniques

4.2.1 Multiple Coherence (MC)

The Multiple Coherence (MC) - which is the multivariate version of MSC - between a periodic signal and a set of *N* random ones ($y_j[k]$, j = 1..*N*) is given by (Miranda de Sá et al., 2004):

$$\hat{\kappa}_N^2(f) = \mathbf{V}^H(f)\hat{\mathbf{S}}_{yy}^{-1}(f)\mathbf{V}(f)\big/M \tag{23}$$

where $\mathbf{V}(f) = \left[\sum_{i=1}^{M} Y_{1i}^*(f) \quad \sum_{i=1}^{M} Y_{2i}^*(f) \quad \cdots \quad \sum_{i=1}^{M} Y_{Ni}^*(f)\right]^T$

being $Y_{ki}(f)$ the Fourier Transform of the i^{th} epoch of the k^{th} EEG derivation; H and T superscripts mean, respectively, Hermitian and the matrix transpose; and the p^{th}-row, q^{th}-column element of $\hat{\mathbf{S}}_{yy}(f)$ is $\hat{\mathbf{S}}_{yp\,yq}(f) = \sum_{i=1}^{M} Y_{pi}^{*}(f) Y_{qi}(f)$.

The distribution of the MC estimates can related to the F-distribution and the critical value for a significance level α, M epochs and N signals can be expressed as (Miranda de Sá et al., 2004):

$$\hat{\kappa}_{N_{crit}}^{2} = \frac{F_{crit\alpha,2N,2(M-N)}}{F_{crit\alpha,2N,2(M-N)} + [M-N]/N} \tag{24}$$

where $F_{crit\alpha,2N,2(M-N)}$ is the critical value of the F distribution with 2N and 2(M-N) degrees of freedom. The detection is identified based on the rejection of the null hypothesis (H_0) of response absence, which is achieved when the estimate values exceed the critical value ($\hat{\kappa}_N^2(f) > \hat{\kappa}_{N_{crit}}^2$). As a multivariate extension of the MSC, MC quantifies the amount of power of a set of signals that is caused by the stimulation.

4.2.2 Multiple Component Synchrony Measure (MCSM)

A multivariate extension of the CSM was proposed by Miranda de Sá and Felix (2003) as a way of measuring the synchronism of the ith epoch of the Fourier Transform of N EEG derivations ($y_1[k]$, $y_2[k]$,…, $y_N[k]$) caused by a rhythmical stimulation only considering their mean phase angle, $\bar{\theta}_i(f)$. This technique, called Multiple CSM (MCSM), can be used for detecting the evoked response and can be mathematically defined by (Miranda de Sá and Felix, 2003):

$$\hat{\rho}_N^2(f) = \left[\frac{1}{M}\sum_{i=1}^{M}\cos\left(\bar{\theta}_i(f)\right)\right]^2 + \left[\frac{1}{M}\sum_{i=1}^{M}\sin\left(\bar{\theta}_i(f)\right)\right]^2 \tag{25}$$

where the M is the number of EEG epochs and the mean phase angle can be calculated by:

$$\bar{\theta}_i(f) = \begin{cases} \tan^{-1}\left(\bar{S}_i/\bar{C}_i\right) & if \quad \bar{C}_i \geq 0 \\ \tan^{-1}\left(\bar{S}_i/\bar{C}_i\right) + \pi & if \quad \bar{C}_i < 0 \end{cases}$$

being

$$\bar{C}_i = \frac{1}{N}\sum_{j=1}^{N}\cos\theta_{ij}(f) \quad \text{and} \quad \bar{S}_i = \frac{1}{N}\sum_{j=1}^{N}\sin\theta_{ij}(f)$$

Assuming that the mean phase angle is uniformly distributed between 0 and 2π, it can be showed, in a similar way to the performed to the CSM, that the asymptotical critical value for the MCSM can be expressed by (Felix et al., 2007):

$$\rho^2_{N\,crit,\alpha} = \frac{\chi^2_{2\,crit,\alpha}}{2M} = \frac{\ln(1/\alpha)}{M} \tag{26}$$

where $\chi^2_{2\,crit,\alpha}$ is the critical value of the chi-squared distribution with 2 degrees of freedom for the significance level *a* and *M* is the number of EEG epochs used in the estimation. Also for this technique, the detection is based on the null hypothesis (H_0) rejection of synchronism absence, which is achieved when the estimate values exceed the corresponding critical value ($\hat{\rho}^2_N(f) > \rho^2_{N\,crit}$).

5. A chronological review of ORD applied to the evoked potentials

The waveform analysis of the evoked potential (EP) is based on the physician experience, ability and attention level, as well as in informal criteria (Dobie and Wilson, 1993). For the case of the somatosensory evoked potential used in surgical monitoring, for example, one considers a significant modification in its waveform, a reduction of 30% to 50% in the amplitude, an increase of 5% to 10% in the latency, or a combination of these criteria (Linden *et al.*, 1997). Such criteria, used as parameters of modification on the intra-operative strategy, are clearly subjective once they depend on the EEG recording quality, anesthesia regimen, and are hampered by the high variability inter-observer and inter-patient (Martin et al., 2002).

On the other hand, the techniques known as Objective Response Detection (ORD) have been suggested as a way to overcome this subjectivity and allow the stimuli-response detection with a maximum false positive rate *a priori* established. Dobie and Wilson (1993) numbered the advantages of the ORD application compared to the conventional analysis by visual inspection, such as avoiding the persistence of the trained observer and obtaining relevant information even for experienced observers in the judgment of questionable cases.

5.1 Univariate ORD techniques

In 1984, Galambos *et al.* (apud Stapells, 1987) introduced the ORD technique Phase Coherence (PC) in the analysis of the steady state auditory responses. This technique can be seen as a statistical measure of the phase variance and uses only the phase information of the Fourier Transform of the EEG epochs. Two years later, Stapells *et al.* (1987) have applied the PC for obtaining the auditory threshold of normal adults. This method showed to be accurate to establish the behavioral auditory threshold, being considered as fast as obtaining the brainstem responses by tones. Moreover, these authors pointed out that the PC showed better results for determining the optimal stimulation rate when compared to the amplitude inspection of the coherent average, since the latter presents higher variability than the PC.

Still in 1987, Picton *et al.* have applied the Hotelling T^2 Test (HT2) and the PC to the steady state auditory evoked potential (AEP). The HT2 (Hotelling, 1931) takes into account both amplitude and phase of the Fourier Transformed EEG epochs and allows the calculation of a confidence ellipse for the response vectors (EP). In the case in which the ellipse do not encompass the origin (0,0), which corresponds to the absence response condition, its presence is assumed (Dobie and Wilson, 1993). Since the PC represents a kind of HT2 without considering the amplitude information (Picton *et al.*, 1987), theoretically, HT2 would

be statistically more powerful than the PC. However, Picton *et al.* (1987) have found small difference between the two methods when the auditory threshold was measured by means of the steady state AEP. Based on these results, the authors have reported that, for intensities near the threshold, most of the information about the signal is in the phase, since using the amplitude information (HT2) didn't result in an improvement in the response detection. Other studies also found that the phase is more important than magnitude (Greenblat *et al.*, 1985, Beagley *et al.*, 1979).

In 1989, Dobie and Wilson have proposed the use of the Magnitude-Squared Coherence (MSC), an ORD technique that uses magnitude and phase of the Fourier Transform of EEG epochs, for identifying the frequencies that significantly contribute to the auditory EP. In this work, the MSC was considered more sensible than the simple visual inspection of the replicated responses. In a later work, Dobie and Wilson (1990) have applied the coherence (MSC) to the AEP filtered with the "Optimum" Wiener Filtering and, compared to the non-filtered version, it was verified that this procedure can be advantageous for signals with low signal-to-noise ratio, such as the obtained with stimulation near the auditory threshold.

Later, Victor and Mast (1991) have proposed a variant of HT2, named T^2 circular (T2C). This method assumes that the real and imaginary parts of the Fourier Transform of the EEG epochs are independent and present equal variance. This assumption results in a simpler statistical approach, and the ellipse of confidence of HT2 becomes a circle of confidence in T2C. Moreover, in this study, a comparison between the performances of three ORD methods was performed: the HT2, the T2C and the Phase Rayleigh Criterion (PRC) – a technique that uses only the phase of the signal. The comparison was based on simulation and application to the steady state visual evoked potential. As a result, it was observed that, for low signal-to-noise (SNR) ratio values, HT2 and T2C have shown to be superior to the PRC. The authors consider that this result is due to the fact that the first two methods use information of amplitude, while the PRC discard it. Furthermore, it was verified that for low SNR, a high number of EEG epochs is needed in order to achieve statistical significance. On the other hand, for a low number of EEG segments, T2C and PRC presented advantage over HT2 and for intermediate SNR values T2C showed better performance than any technique.

Dobie and Wilson (1993) also compared the performance of T2C, PC and MSC using simulated signals. Additionally, a variant version of the MSC, the MSC-WA (WA, of Weighted Averaging), which consists of the multiplication of each epoch by the inverse of its power, was investigated. This weighting assumes that epochs with high power are the ones that present lower SNR and, therefore, should have their weight reduced. This procedure can be particularly interesting in the cases of non-stationary noises, which can harm the performance of the MSC, leading it to have inferior results to the PC (Dobie and Wilson, 1993). According to these authors, the T2C is mathematically related to the MSC, and it is possible to obtain one estimator from the other, although the MSC is computationally simpler. The MSC (or T2C) weighted averaging was the technique that presented the best performance in the detection of response to the auditory stimulus. In a later study (Dobie and Wilson, 1994a), the MSC, the MSC-WA and the PC were applied to the steady state 40Hz AEP. The three techniques presented similar performance in the response detection, although a slightly advantage for the MSC-WA over the MSC and for the MSC over the PC has been observed (Dobie and Wilson, 1994b).

At the same year, Dobie and Wilson (1994b) have applied the MSC and the MSC-PW (PW, of Phase Weighting) to the steady state 40Hz AEP. In the MSC-PW, a weighting is applied and it is related to the phase error calculated as the difference between the phase of the averaged signal (coherent average) and an expected phase (or target-phase). The target-phase is calculated from the coherent average with a high M number of EEG epochs during stimulation with intensities higher than the commonly used for obtaining the AEP. As a result, it was verified that the phase weighting improved the performance of the MSC. At the same year, Miranda de Sá et al. (1994) investigated the theoretical confidence limits for the coherence estimate (MSC) comparing them to the limits obtained by simulation with random signals.

In 1995, Dobie and Wilson (1995) verified the superior performance for the MSC-WA, when compared to the human inspection. The MSC-WA allowed detecting the responses to auditory stimulation with a lower number of stimuli and with lower stimulation intensity. At the same year, Thakor *et al.* (1995) have proposed an adaptive algorithm for the coherence estimate, in order to detect changes in the somatosensory evoked response. This study showed that, during hypoxia in cats, the MSC presents a sharp decrease, confirming the applicability of the adaptive MSC for monitoring purposes.

In 1996, Dobie and Wilson (1996) compared the Spectral F Test (SFT) and the MSC in the detection of the steady state AEP and concluded that, as they presented the same performance, the choice for using one technique or other would be a convenience issue. Two years later, Liavas *et al.* (1998) used successfully an ORD technique based on the periodogram for detecting the steady state visual evoked potential, aiming at investigating neuropathies related to the visual system.

Applying a decreasing exponential weighting to the spectral estimates of the EEG epochs during somatosensory stimulation used for MSC calculation, Tierra-Criollo *et al.* (1998) showed that this technique leads to the detection of the evoked responses faster than its simple version. This weighting emphasizes the latest spectral estimates, making the MSC more representative of the current status of the patient. This technique was named MSC with exponential forgetting (MSC-EF). Due to its promising results, Tierra-Criollo (2001) suggested the application of both the MSC and MSC-EF to the posterior tibial nerve SEP as a method to be evaluated for real-time monitoring of surgical procedures.

In 2000, Ramos et al. compared the MSC and the CSM (Component Synchrony Measure), which corresponds to the square of the PC (Phase Coherence). They reported that there is no statistical difference in performance for response detection when applied to the EEG of children and newborns during click stimulation. However, the MSC showed higher specificity in the detection of auditory deficiency, which gives to this technique greater clinical interest. Moreover, this method presented higher potentiality for determining the auditory threshold in the studied age group (Ramos et al., 2000). Also in the detection of the somatosensory response, the MSC presented better performance when compared to the CSM and the SFT (Simpson *et al.*, 2000, Tierra-Criollo, 2001). The MSC was also applied to the EEG during intermittent photic stimulation in order to quantify the degree of cortical activation (Miranda de Sá, 2000) and in the identification of inter-hemisphere symmetry between homologues regions of the visual cortex at the stimulation frequency and its harmonics (Miranda de Sá and Infantosi, 2002).

Miranda de Sá *et al.* (2001) proposed a coherence-based method to emphasize the stimuli-synchronized responses and reduce the background EEG influence. Later (Miranda de Sá *et al.*, 2002), the confidence limits for the coherence estimates between one random and one periodic signal were calculated based on a monotonically increasing function of the estimates, which involves the non-central F-distribution. Miranda de Sá (2004) obtained the sampling distribution of this coherence estimate itself and found it to be non-central beta distributed. This allowed further investigations to be carried out (Miranda de Sá *et al.*, 2009) for assessing both bias and variance of the estimate as well as the performance of the normalizing transform in it.

The MSC and the CSM were also applied for monitoring the anesthetic plan (Cagy *et al.*, 2000, Cagy, 2003). These studies showed that, during infusion of anesthetic, a reduction in values of both estimates is verified. Moreover, the results for MSC and CSM were quite similar, indicating the phase to be more important than the magnitude, as previously reported by Dobie and Wilson (1993). The MSC was also used to identify the maximum response band for the Brainstem Auditory Evoked Potential (BAEP) (Pacheco, 2003, Pacheco and Infantosi, 2005).

Infantosi *et al.* (2004) applied the MSC to the Middle Latency Auditory Evoked Potential (MLAEP) of normal individuals for different sound pressure levels aiming at investigating the frequency bands that better characterize this evoked response for distinct stimulation intensities. They have found consistent response detection for frequencies within the gamma band (30-50 Hz). Furthermore, the application of the MSC to the AEP for determining the auditory threshold L, defined as the volunteer response to a click stimulation, resulted in the detection near the visual identification by a specialist of the BAEP waves (L and L+5) or of the MLAEP's (L+15).

Melges *et al.* (2005) employed the methodology suggested by Tierra-Criollo (2001), and used the temporal evolution of the MSC for a given frequency in order to evidence the transitions from tibial nerve somatosensory stimulation to resting condition, and conversely. The transition from a responsive to a no-responsive status is very important for surgical monitoring and this work have mimicked these statuses by presenting and omitting the stimulus. At the same year, Miranda de Sá *et al.* (2005) have investigated the coherence between two EEG derivations due to a visual rhythmic stimulation and the partial coherence (after removing the contribution of the stimulus) applied to the same signals. They concluded that these techniques present complementary role, since the coherence quantifies the degree of synchronism between the derivations, whereas the partial coherence informs about the relationship due to the non-phase locked activities, suggesting its use in ERD/ERS (event related desynchronization/synchronization) studies.

In 2006, Campos *et al.* (2006) applied the SFT to the EEG of epileptic patients during intermittent photic stimulation, and concluded that this technique should be employed as a complement to the traditional identification methods of photo-recruited responses, such as spectral analysis. By using EEG signals during the same type of stimulation, Miranda de Sá *et al.* (2006) studied the SFT applied to the signals of normal individuals. Moreover, they investigated the probability distribution of this test, as well as the confidence limits for its estimates, using simulated signals with different signal-to-noise ratio and *M*-values. Since the majority of the EP applications use periodic stimulation (intermittent photic stimulation, train of current pulses or clicks), Miranda de Sá (2006a) developed analytical expressions for calculating the trend, variance and probability density function for the coherence (MSC), in the particular case in which the input signal (stimulus) is periodic.

Tierra-Criollo (2001) and Infantosi *et al.* (2006), by applying the MSC to the responses evoked by electric stimulation, identified the low gamma band (30-60 Hz) as the one that better represents the short-latency components of the somatosensory evoked potential. Also in 2006, Klein *et al.* (2006) have introduced a variant of the MSC, the Wavelet Coherence (WC), which allowed obtaining the temporal information that is lost when frequency-domain techniques are used.

Infantosi and Miranda de Sá (2006) proposed a methodology based on the MSC in order to study EEG activities that are synchronized in time (time-locked) with the stimulation signal, but non-synchronized in phase (non phase-locked). Such technique was investigated using the visual evoked potential, elicited by intermittent photic stimulation. In another study, Miranda de Sá (2006b) developed an expression for the partial coherence between two signals, removing the contribution of the stimulation, and showing that this estimates is independent of the stimulus signal. In 2007, Miranda de Sá and Infantosi (2007) introduced a method based on the estimates of the MSC and the Partial Coherence in order to quantify the similarity between two EEG activities that are not synchronized in phase with the stimulation signal. At the same year, Cagy and Infantosi (2007) showed that the MSC is capable of indicating modification both in amplitude and latency of the MLAEP.

Later, Melges *et al.* (2008a) investigated the topographic distribution of the tibial nerve somatosensory evoked potential (SEP) using the MSC and verified that the best regions for SEP recording, in an ORD approach, includes the central and parietal leads at the midline and parasagittal line ipsilateral to the stimulated limb. Two years later, Farina *et al.* (2010) proposed a novel ORD technique based on the Rice distribution, obtaining the analytical critical values and using simulated signals to calculate the probability of detection for different values of signal-to-noise ratio.

More recently, Melges *et al.* (2011a) showed that, although the variation of the stimulation frequency to values higher than 5 Hz produces distortion in the tibial nerve SEP waveform, hampering the visual inspection, the detection rates obtained with the MSC (and CSM) are statistically equivalent for different stimulation frequencies. Hence, higher values can be used in order to fasten the detection. The maximum frequency, however, is limited to about 10 Hz, since higher values could lead to steady state tibial nerve SEP, instead of transient one.

5.2 Multivariate ORD (MORD) techniques

The introduction of the ORD techniques represented an advance in the study of the evoked potentials, since these methods are based in statistical tests for inferring about the absence of stimulus-response (Dobie and Wilson, 1989). These techniques present the advantage (over traditional methods of identification of response), since they have a maximum false-positive rate (false alarm) a priori defined. However, for a fixed signal-to-noise ratio, it is only possible to improve the response detection rates, at the expense of increasing the recording length (number M of EEG epochs). This aspect may limit the application of ORD techniques, especially for surgical monitoring, case in which a fast detection of EP variations is needed, aiming at modifying the intra-operative strategy to avoid the occurrence of neurological damages.

In order to overcome this drawback and improve the detection rates, Miranda de Sá and Felix (2002) suggested the employment of multivariate extensions of the ORD techniques,

named MORD (Multivariate ORD), which use information of more than one EEG derivation. In this study, they introduced the Multiple Coherence (MC), a multivariate version of the MSC, and verified that the detection percentages can be improved by augmenting the number of EEG channels used. These authors also verified that, similar to the proved to the uni-variate version (MSC), the estimate of the MC, for a periodic and deterministic stimulation, is independent of the stimulation signal. Moreover, they showed, by means of simulation, that even the addition of a second EEG signal with lower signal to noise-ratio than the first could result in an increase in the probability detection. Since the MORD does not require increasing the number of epochs for obtaining higher detection rates, the MC has been suggested as a useful tool to be applied in the surgical monitoring, allowing a faster detection of the elicited responses.

In the following year, Miranda de Sá and Felix (2003) proposed a multivariate extension for the Component Synchrony Measure (CSM), the MCSM (Multiple CSM), for which it was verified that the detection rates for the intermittent photic stimulation responses increase by augmenting the number of signals used in its calculation. Such results were observed for both simulated and real EEG signals.

In 2004, Miranda de Sá *et al.* (2004) proposed a matrix-based algorithm for the calculation of the Multiple Coherence. The results obtained by simulation showed that for achieving a detection probability of 95%, for example, the signals added to the set of EEG channels used for the MC estimate can present SNR lower than the first one. This can be observed until the 6^{th} signal, from which a signal with SNR higher than the first one should be employed in order to maintain the detection rate (95%). However, in this case it would be more advantageous using only the 6^{th} signal for estimating the MSC.

Later, Ferreira and Miranda de Sá (2005) compared the simple, multiple and partial coherences applied to the EEG during intermittent photic stimulation and consider these techniques promising in the analysis of the EEG during sensory stimulation. In the same year, Infantosi *et al.* (2005) verified, as theoretically predicted (Miranda de Sá and Felix, 2002, Miranda de Sá *et al.*, 2004), a better performance of the MC when compared to the MSC applied to the EEG during somatosensory stimulation of the tibial nerve. In this study, the MSC was applied to the bipolar derivations [Cz'-Fpz'] and [C3'-C4'] (where [Fpz'] is midway between [Fpz] and [Fz]; [Cz'], [C3'], and [C4'] are 2 cm posterior to [Cz], [C3] and [C4], respectively) - very often used for scalp SEP recording - and the MC was applied to both derivations. Using EEG signals from the same derivations during electric stimulation, Melges *et al.* (2006a) have found the MCSM to be useful for tibial nerve SEP detection. At the same year, Melges *et al.* (2006b) compared the performance of the MC and the MCSM, observing higher detection rates for the former. This result was observed for different values of M epochs (100, 200, 400, 800) used in the calculation of the estimates. A comparison between the two techniques applied to the EEG during intermittent photic stimulation (Felix *et al.*, 2007) has also resulted in higher detection percentages for the MC over the MCSM. By means of simulation, it was observed that the presence of noise correlated with the responses degrades the detection rates (Felix *et al.*, 2007).

In 2008, Miranda de Sá *et al.* (2008) derived the probability density function of the MC and a set of evoked responses embedded in additive noise for the zero-coherence case (null hypothesis of response absence). In this work, it was also demonstrated the influence of the

number of EEG epochs (*M*) in both bias and variance of the MC estimates. At the same year, Melges *et al.* (2008b) compared the performance of MSC applied to the bipolar derivations [Cz-Fz] and [C3-C4] with the MC applied to the pairs of unipolar derivations [Cz][Fz] and [C3][C4]. The results showed that if two leads are available, it is better to use the MC of unipolar recordings than the MSC applied to the difference of the leads (bipolar derivation).

Since the use of unipolar derivations seemed to be more adequate, the performance for the MC and MCSM were compared, by applying both techniques to the pairs of unipolar derivations [Cz][Fz] and [C3][C4] (Melges *et al.*, 2010). The comparison was performed for *M*=100 and 800 epochs. The MC outperformed the MCSM, regardless the pair of derivations or the number of EEG epochs used for the estimates calculation.

More recently, Melges *et al.* (2011b) compared the MSC applied to the unipolar derivations [Cz], [Fz], [C3] and [C4] - usually employed in a bipolar SEP recording, as above mentioned - and the MC applied to the pairs [Cz][Fz] and [C3][C4]. The results evidenced the detection improvement by using synergically the information of two derivations, showing to be more advantageous using the MC than the MSC.

6. Examples and applications of ORD and MORD techniques

This section presents examples of using ORD and MORD techniques to the EEG during somatosensory stimulation. Following, the experimental protocol of EEG acquisition, the pre-processing and processing steps, and some results are shown.

6.1 EEG acquisition, pre-processing and processing

EEG Acquisition: EEG signals during somatosensory stimulation were collected from forty adult volunteers aging from 21 to 41 years old (mean ± standard deviation: 28.6 ± 4.6 years), without history of neurological pathology and with normal SEP. The signals were collected using the EEG BNT-36 (EMSA, Brazil, www.emsamed.com.br) according to the 10-20 International System and all leads referenced to the earlobe average. The volunteers were laid down in the supine position with eyes closed. The stimuli were applied by means of current pulses (200 μs width) to the right posterior tibial nerve using the Atlantis Four (EMSA, Brazil, www.emsamed.com.br). About 1000 to 1400 stimuli were applied at the motor threshold (the lowest intensity that produces toe oscillations) and at the rates of 1.99, 4.83, 6.68, 8.51 Hz (nominal values: 2, 5, 7, 9 Hz). The motor threshold was determined by an accelerometer tied in the toe that allowed the recording of the oscillations. The stimuli in the frequencies of 7 and 9 Hz were applied to 32 of the 40 volunteers. The ground electrode was attached to the poplitea fossa. Surface silver and gold electrodes were used, respectively, for recording and stimulation. An Institutional Review Board approved this research and all volunteers signed informed consent forms.

Pre-processing: The signals were band-filtered (0.5 – 100 Hz) and digitized (16-bits resolution) with BNT-36 at the sampling rate of 600 Hz. Then, the EEG was segmented into epochs of 501, 207, 149 and 117 ms, stimuli-synchronized, leading to spectral resolution of 2.0, 4.83, 6.71 and 8.55 Hz, respectively. In order to minimize the interference of the stimulus artifact in the ORD and MORD techniques we have set to zero the first 5 ms after each stimulus. Furthermore, the final 5 ms were zero padded to ensure window symmetry. A Tukey window with 7 ms rising (falling) time has been next applied to each

epoch to ensure that the late components of the artifact are also attenuated. Noisy epochs were next discarded by a semi-automatic artifact rejection algorithm, which rejects epochs with more than 5% of continuous samples or more than 10% of samples exceeding ± 3 SD (where SD is the standard deviation of 20 s of noise-free background EEG selected as reference signal). Details about the windowing and artifact rejection can be found in Infantosi *et al* (2006).

ORD and MORD application: $\hat{\kappa}^2(f)$, $\hat{\kappa}^2_{crit}$, $\hat{\kappa}^2_N(f)$, $\hat{\kappa}^2_{N\,crit}$, $\hat{\rho}^2(f)$, $\hat{\rho}^2_{crit}$, $\hat{\rho}^2_N(f)$, $\hat{\rho}^2_{N\,crit}$ were calculated for the EEG signals using expressions (9),(11),(23),(24),(18),(20), (25), (26), respectively. The significance level $\alpha = 5\%$ was generally adopted, but the *M*-value varied and is cited for each illustration that follows. The detection was achieved when the estimate values exceeded the critical value.

6.2 The tibial nerve somatosensory evoked potential waveform

As mentioned in the Section 2, the waveform quality of SEP is very dependent on the number of stimulus presented. Figure 2 illustrates this characteristic of the analysis performed by visual inspection. For the coherent average obtained with *M*=50 epochs for derivation Cz of volunteer #35, the tibial nerve SEP waveform is very noisy and it is difficult to identify its characteristic waves. For *M*=200 epochs, the P37 (at 40 ms) and N45 (at 52 ms) are visible, respectively with amplitudes equal to -2.86 μV and 0.86 μV. However, it can be seen that, when a higher number of epochs (*M* = 500 epochs) is used, the waveform is smoother and the identification of the short-latency SEP components can be easily pointed even for an untrained observer at 40 ms and 50 ms.

Even for the SEP obtained with high signal-to-noise ratio, the components P37 and N45 presents high amplitude and latency (time duration from the stimulus to a peak or valley occurrence) variability, as it can be observed in Figure 3, which presents the SEP for six individuals calculated by averaging 500 epochs. This variability, associated with low signal-to-noise SEP recording obtained in hospital units, reinforces the subjectivity of such analysis.

6.3 ORD techniques applied to the somatosensory evoked response detection

The application of MSC to the EEG of volunteer #40 (stimulated at 6 mA) is illustrated in Figure 4. The horizontal black dashed line represents the detection threshold; when the corresponding MSC tracing surpasses its critical value, the detection is assumed for that (those) specific frequency (frequencies). As it can be observed, the MSC presents low values for derivation [C3] and higher values for [C4], that is, the higher response effects occur ipsilateral to the stimulated limb (the well known paradoxical lateralization (Cruse et al., 1982)). For derivation [C4], the detection is evident, predominantly at the frequencies from 30 to 65 Hz. On the other hand, for [C3], MSC exceeds the critical value only for the frequencies 29.0 and 33.8 Hz (nominal values: 30 and 35 Hz).

Both the CSM and MSC of derivation [C4] of volunteer #38 are showed in Figure 5, in which it can be visualized the similarity of values of $\hat{\rho}^2[C4]$ and $\hat{\kappa}^2[C4]$. Since the CSM can be obtained from the MSC when the amplitude information is discarded, this similarity evidences the importance of phase in the Objective Detection.

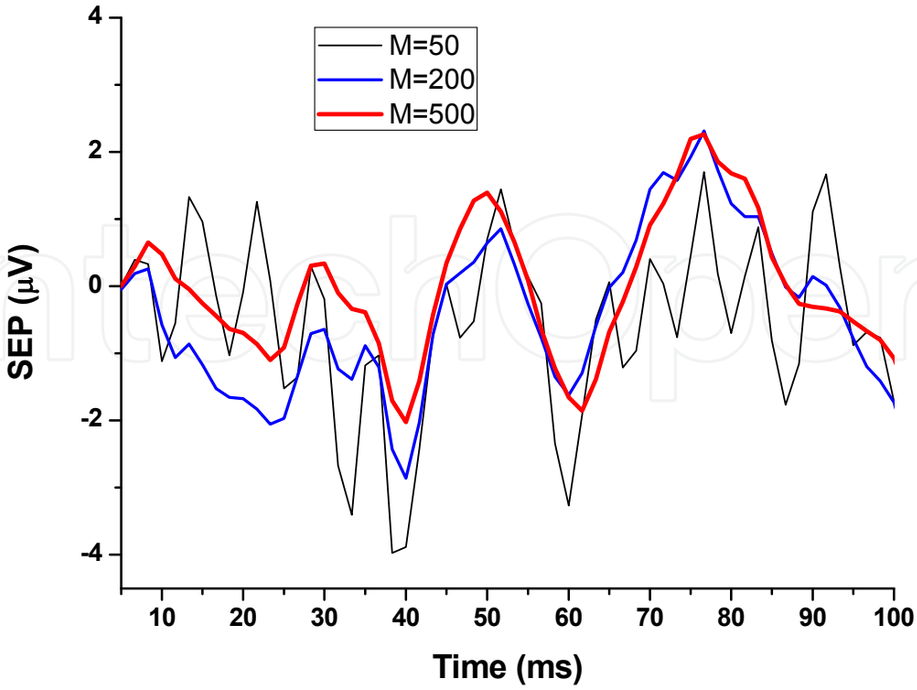

Fig. 2. Coherent Average (M = 50, 200 and 500 epochs) of derivation [Cz] of volunteer #35, stimulated at 24 mA and 5 Hz.

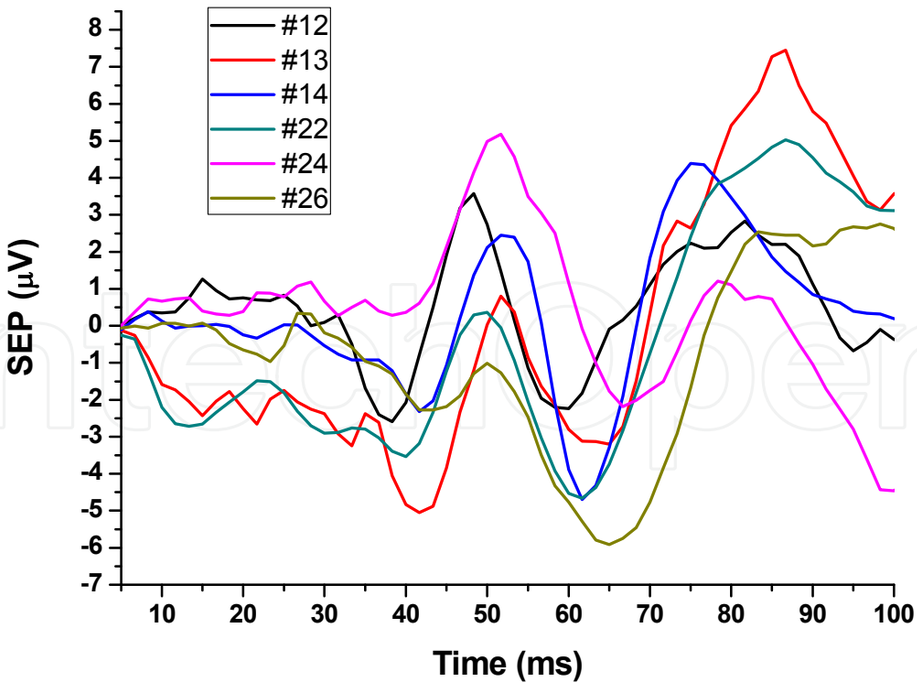

Fig. 3. Coherent Average (M = 500 epochs) of derivation [Cz] of volunteers #12, #13, #14, #22, #24, #26, respectively stimulated at 10, 10.5, 18, 12.5, 16 and 15 mA (these currents correspond to the individual motor threshold) and 5 Hz.

As it should be clear, establishing a statistical threshold for identifying the response detection reduces the subjectivity of the analysis. It is worth noting that the maximum false positive alarm can be as lower as desired, setting up α for the corresponding value.

6.4 Topographic distribution of the evoked responses

The localization on the scalp of the response to a specific kind of stimulation is a critical issue for the detection performance, since it determines the best regions for the evoked potential recording. In Melges et al. (2008), we have described that the leads with best signal-to-noise ratio for electrical stimulation of the right posterior tibial nerve are [Pz], [P4], [Cz], [C4] that is, leads at the parietal and central regions midsagital and ipsilateral to the stimulated limb. The results were obtained with the MSC applied to the SEP using 5 Hz as frequency of stimulation (f_{stim}). In fact, although the SEP is known to change its waveform characteristics with the stimulation frequency, the best detection percentages were obtained in the same leads for all investigated frequencies (2, 5, 7 and 9 Hz). Figure 6 shows the performance of the MSC for all the casuistry stimulated at the motor threshold and with f_{stim} = 9 Hz. As it can be seen, the same leads [Pz], [P4], [Cz], [C4] present the best detection rates. The ordinate presents the percentage of volunteers for whom it was possible to detect the evoked response for each frequency from the 1st to 12nd harmonics of the stimulation frequency.

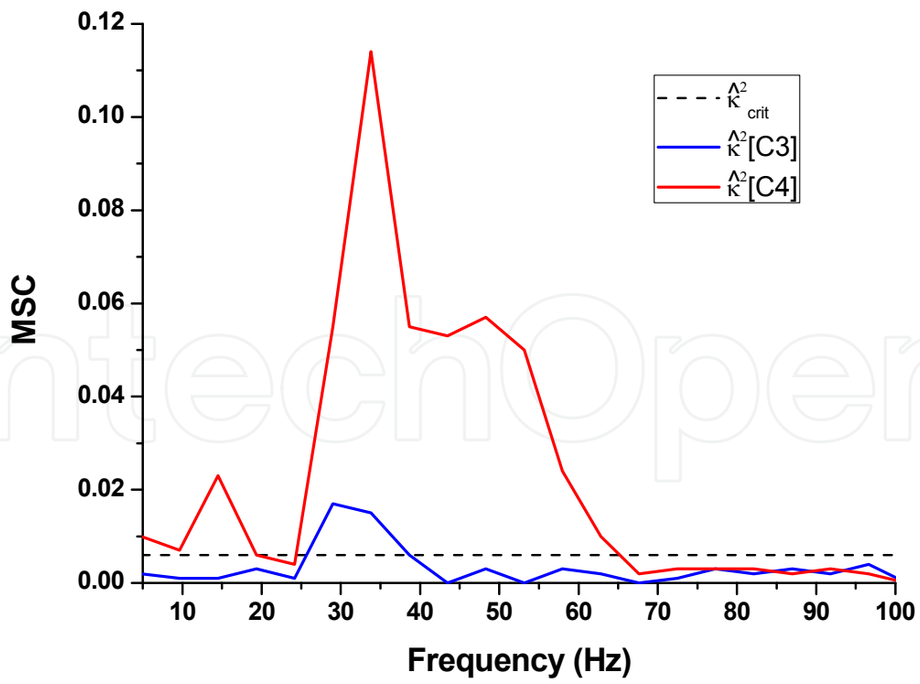

Fig. 4. $\hat{\kappa}^2[C3]$ and $\hat{\kappa}^2[C4]$ of volunteer #40, stimulated at 6 mA and 5 Hz. Horizontal line represent the critical value: $\hat{\kappa}^2_{crit} = 0.006$ (M = 500 epochs and α=0.05). Vertical axis (MSC) is dimensionless.

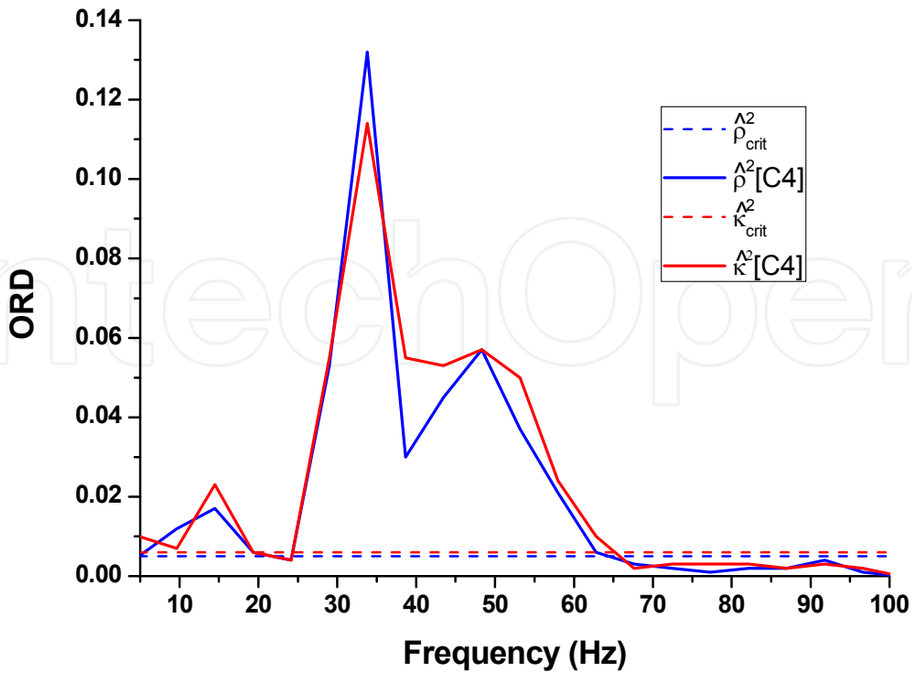

Fig. 5. $\hat{\rho}^2[C4]$ and $\hat{\kappa}^2[C4]$ of volunteer #38, stimulated at 14 mA and 5 Hz. Horizontal lines represent the critical values: $\hat{\rho}^2_{crit} = 0.005$ and $\hat{\kappa}^2_{crit} = 0.006$ (M = 500 epochs and α=0.05). Vertical axis (ORD) is dimensionless.

6.5 Maximum response frequency band

Apart from choosing suitable sites for EP recording, selecting the frequencies that are more responsive to a specific kind of stimulation is also important, since it leads to a more reliable objective neurophysiologic evaluation during surgical procedures.

From Figure 6, it is also possible to identify, in the derivations with best detection percentages, that the frequency range that includes from 2nd to the 6th harmonics of the stimulation frequency (9Hz) - frequencies from 18 to 54 Hz - is the more responsive. Hence, the presence of stimuli-response leads to positive detection in these frequencies, which were classified as the maximum response frequency band (Tierra-Criollo, 2001, Infantosi *et al.*, 2006); that is, frequencies within this range should be selected in order to augment the probability and rapidness of detection.

6.6 Stimulation frequency

The increase of the stimulation frequency is the simplest way of obtaining faster the response to a set of M stimuli, and enhances the time of detection. However, this frequency increase is known to cause changes in the SEP waveform (Chiappa, 1997, p. 307 and 323), whose characteristics are the basis for neurophysiologic monitoring. Fortunately, the detection rates obtained with an ORD approach is not statistically modified for different stimulation frequencies, as it was shown in a recent study of ours

(Melges *et al.*, 2011a). In this case, the use of the higher investigated frequency 9 Hz, represent a gain of 9:5 in the time of detection, if we consider the very often used stimulation frequency (5 Hz). Figure 7 presents the detection rates for derivation [Cz] and *M* = 200 epochs. In this figure it is possible to visualize the similarity in the profile of the detection percentage tracings, showed to be statistically equivalent for the maximum response frequency band, for both M = 100 and 500 epochs (Melges *et al.*, 2011a).

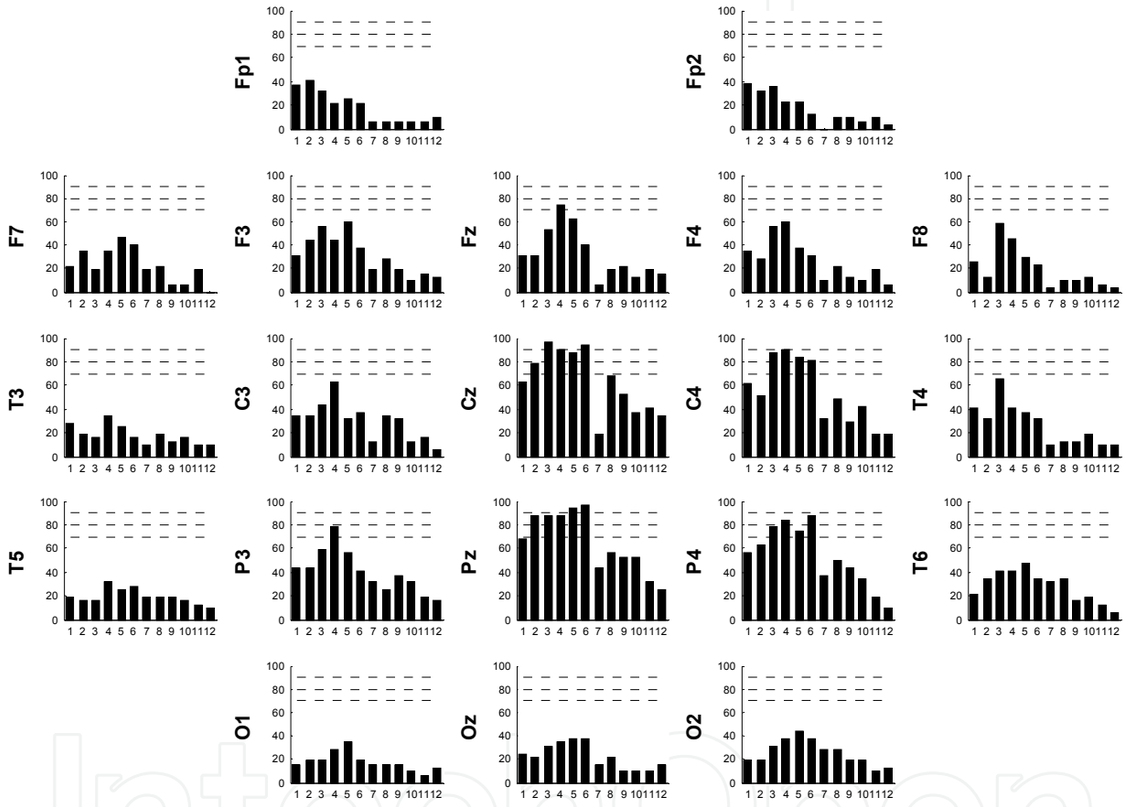

Fig. 6. Percentage of volunteers whose response to the stimulation could be detected using the MSC for multiples from 1 to 12 (9 to 100 Hz) of the stimulation frequency (9 Hz). Horizontal lines indicate 70, 80 and 90% of detection. For derivations Fp2 (31), F8 (31) and C4 (31), it was not possible to obtain 500 artifact-free epochs for the 32 volunteers, hence, the percentages were calculated with the number of volunteers in parenthesis.

6.7 ORD temporal evolution

After identifying the more responsive frequencies and have optimized the stimulation frequency aiming the fast detection, it is possible to choose one or some frequencies for monitoring its temporal evolution. In Figure 8A, a modulus of a Virtual Instrument

(software) for Evoked Potential Objective Detection developed in Melges (2005) is shown, containing the temporal evolution of the MSC for the frequency of 36.8 Hz (Horizontal line represents the detection threshold). This signal was collected from volunteer #6, using parameters very commonly applied during surgical procedures. That is, the EEG was collected from derivation [Fpz'-Cz'] and with stimulation frequency of 5 Hz. In order to evaluate the capability of the MSC to reflect the transition of a responsive status to a no-responsive one, these conditions were mimicked by periods with and without electrical stimulation, respectively. Moreover, four periods with stimulation (S) were alternated with no-stimulation (NS) periods (starting without stimulation). The first S-period corresponds to the stimulation with the motor threshold intensity level (MT). In the following three S-periods, an intermediary intensity (IT) level was used; this intensity value was obtained by the arithmetic mean between MT and the sensitivity threshold, which corresponds to the lowest current level that is felt by the individual.

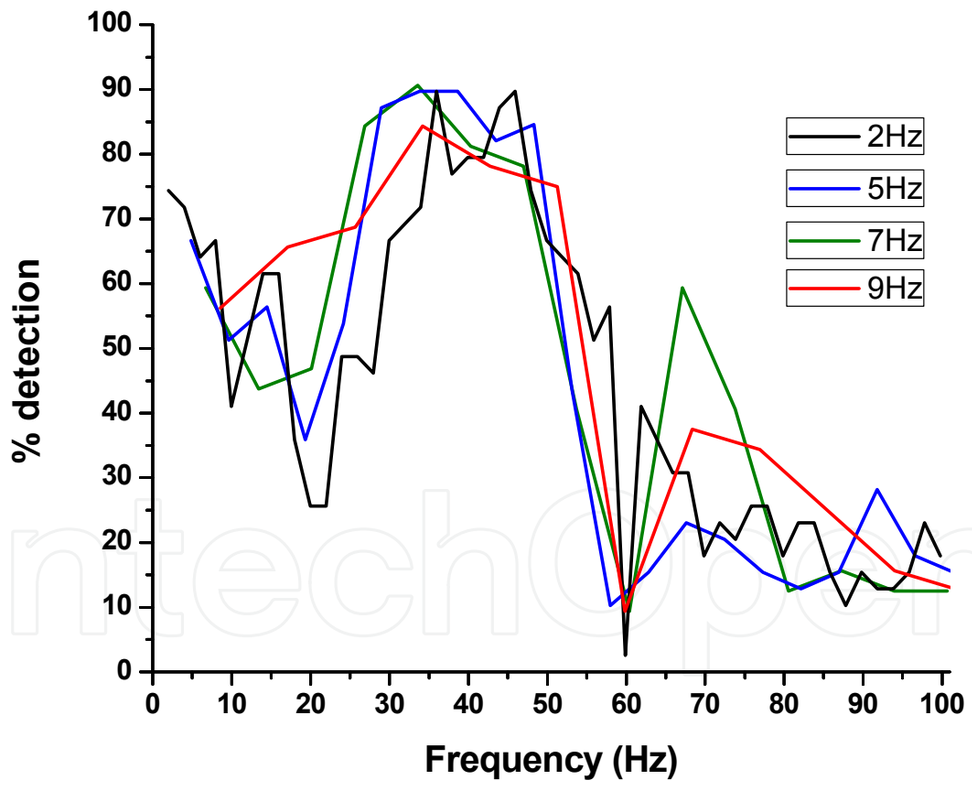

Fig. 7. Percentage of volunteers for whom the stimulation response was detected using the MSC (M = 200 epochs) for the frequencies from 2 to 100 Hz at the derivation [Cz] for the stimulation frequencies 2, 5, 7, 9 Hz.

The MSC estimates can be dynamically estimate as follows: 1) Store M EEG epochs in a matrix (A_{EEG}); 2) Calculate the MSC estimate using the M EEG epochs of A_{EEG} and

expression 9; 3) When a new EEG epoch is acquired, substitute the older EEG epoch of A_{EEG}, i.e., the first line of it, by the new epoch and return to step 1.

From Figure 8A, one can note that even for a low *M*-value (*M*=50 epochs), the MSC was capable to follow the transition from rest to stimulated condition (Figure legend indicates the instant when the stimulus started and stopped), and conversely. Since the increase of *M* is known to improve the detection rate, the time evolution of MSC was also evaluated using *M*=400 epochs (Figure 8B). As it can be noted, the MSC estimate with *M*=50 epochs (MSC_{M50}) presents higher variability than the obtained with *M*=400 epochs (MSC_{M400}). On the other hand, MSC_{400} presents a higher inertia to change from one status to the other. Hence, the *M*-value should be parsimoniously chosen for the clinical or intra-operative application.

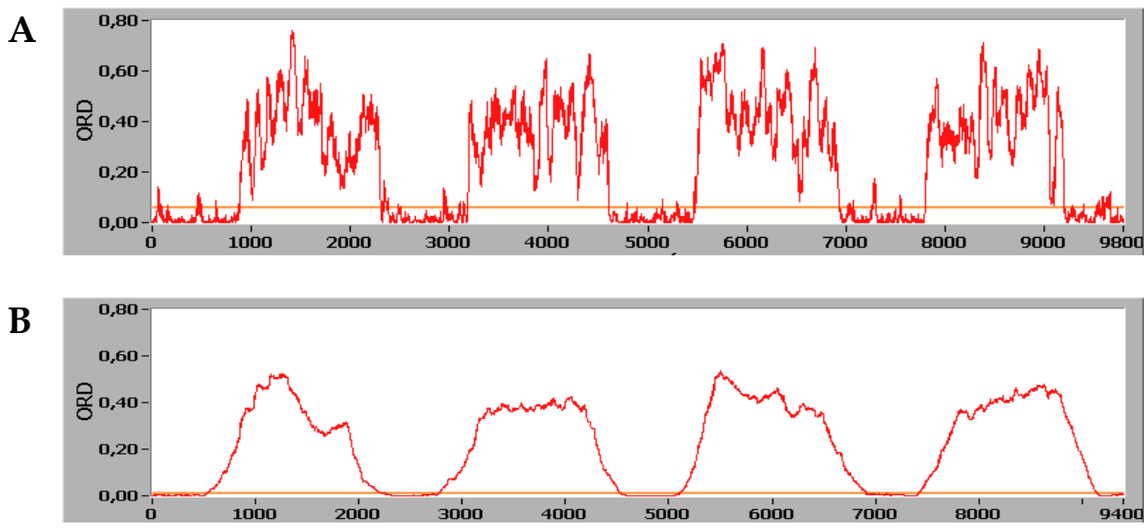

Fig. 8. $\hat{\kappa}^2(f)$ of the frequency 36.8 Hz (α=0.05) for derivation [Fpz'-Cz'] of volunteer stimulated at MT and IT for A) *M*=50 epochs (Horizontal orange line: $\hat{\kappa}^2_{crit} = 0.0593$); B) *M*=400 epochs ($\hat{\kappa}^2_{crit} = 0.0075$). Transitions from/to stimulated to/from no-stimulated condition at: A) t=830, 2296, 3164, 4591, 5459, 6889, 7781 and 9204 elapsed epochs. B) t=480, 1946, 2814, 4241, 5109, 6539, 7431 and 8854 elapsed epochs. Horizontal scale in elapsed epochs. Vertical axis (ORD-MSC) is dimensionless. The decimal separator in the coordinates scale is "comma", since the virtual instrument was developed using Brazilian Portuguese Regional Settings.

6.8 MORD techniques applied to SEP

The use of more than one derivation, as suggested by Miranda de Sá and Felix (2002), can improve the detection rates without the need of augmenting the exam duration (the number of EEG epochs used for ORD estimation). Figure 9 shows the MSC (*M* = 100 epochs) for [C3] and [C4], and the MC (*M* = 100 epochs) using both leads of volunteer #17. Since the somatosensory region on the contralateral hemisphere presents SEP with very low

amplitude, as expected, the MSC values are low and under the detection threshold. On the other hand, the lead ipsilateral to the stimulated limb, [C4], shows detection for the nominal frequencies 35, 40, 50-60 Hz. It is worth noting that the employment of the $\hat{\kappa}_2^2[C3][C4]$ resulted in estimate values higher than $\hat{\kappa}^2[C3]$ and $\hat{\kappa}^2[C4]$, and the MC tracing surpasses its corresponding critical value for 35-60 Hz.

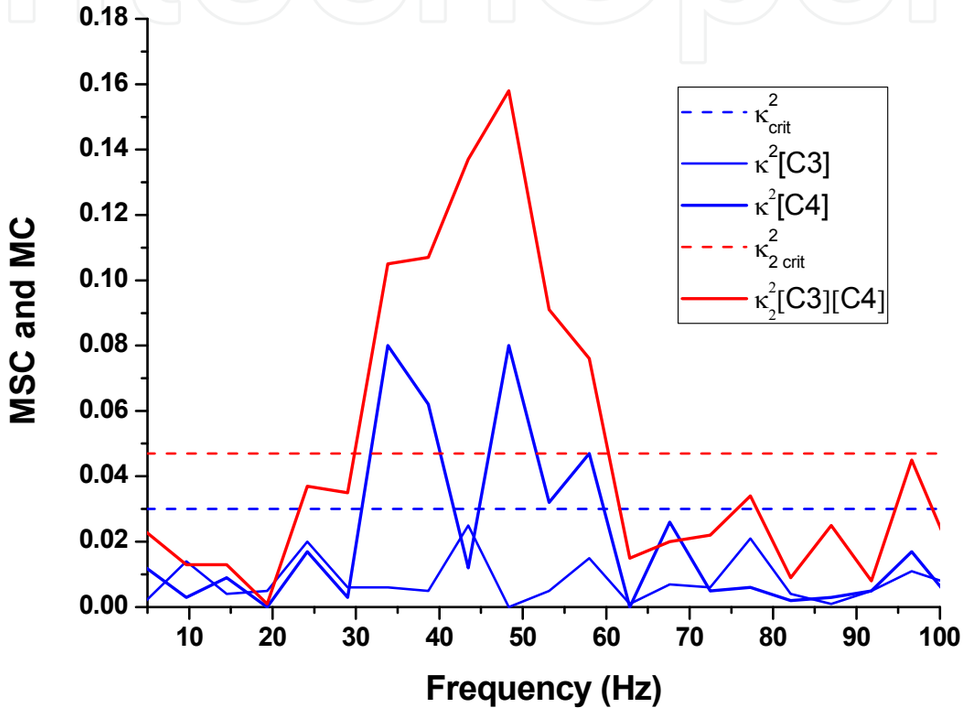

Fig. 9. $\hat{\kappa}^2[C3]$, $\hat{\kappa}^2[C4]$ and $\hat{\kappa}_2^2[C3][C4]$ of volunteer #17, stimulated at 10 mA and 5 Hz. Horizontal lines represent the critical values: $\hat{\kappa}_{crit}^2 = 0.0300$ and $\hat{\kappa}_{2crit}^2 = 0.0470$ for α=0.05, M = 100 epochs and N=2. Vertical axis (MSC and MC) is dimensionless.

The detection rates for the MSC applied to [Cz] and [C4] and for MC applied to [Cz][C4] is showed in Figure 10A. It is easy to note that the percentages for $\hat{\kappa}^2[Cz]$ are higher than the observed for $\hat{\kappa}^2[C4]$, and both are lower than $\hat{\kappa}_2^2[Cz][C4]$. Hence, "adding" the information from [Cz] to the [C4] resulted in an increase in the overall response detection performance.

In fact, even when a derivation with lower signal-to-noise ratio ([C3]) is added to the estimation of the Multiple Coherence, the detection rates can be improved (Figure 10B), as theoretically predicted by Miranda de Sá and Félix (2002).

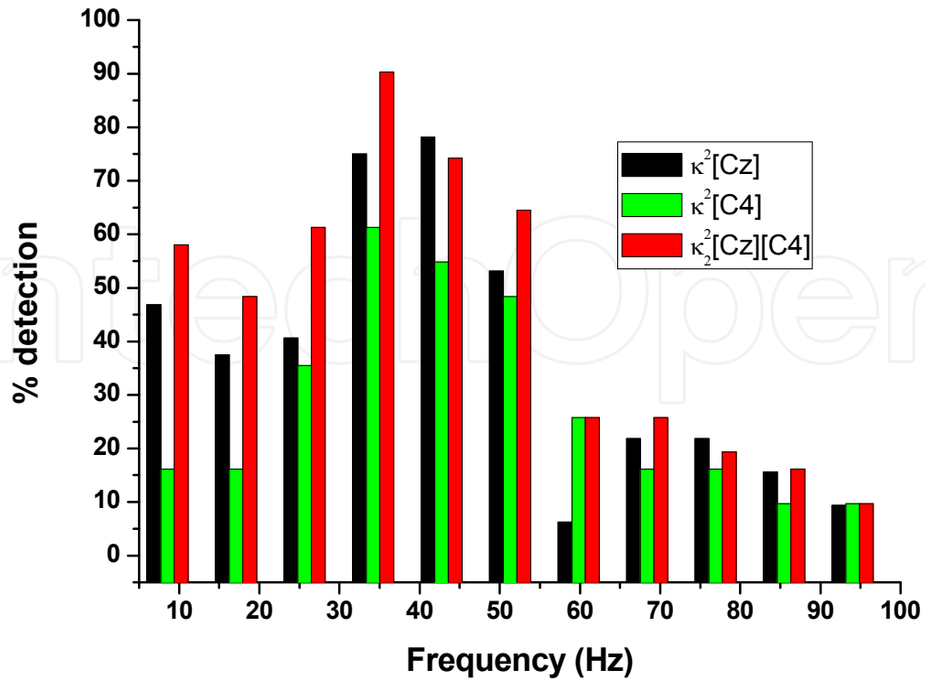

A

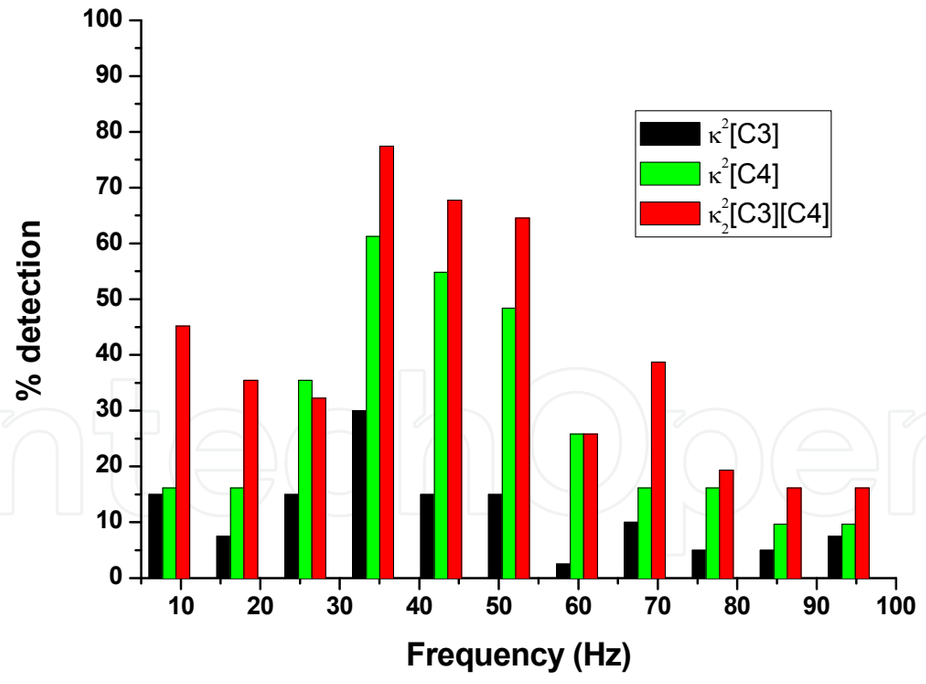

B

Fig. 10. Detection rates (M = 100 epochs) for A) $\hat{\kappa}^2[Cz]$, $\hat{\kappa}^2[C4]$ and $\hat{\kappa}_2^2[Cz][C4]$; B) $\hat{\kappa}^2[C3]$, $\hat{\kappa}^2[C4]$ and $\hat{\kappa}_2^2[C3][C4]$. For derivation [Cz], it was only possible to obtain 100 artifact-free epochs for 39 from the 40 volunteers, hence, the percentages of detection for [Cz] and [Cz][C4] were calculated over 39.

7. Conclusion

The ORD approach allows the detection of sensory response with a maximum false-positive rate (α) that can be defined as strict as desired. This leads to techniques that can be employed for a variety of occasions ranging from children auditory screening to the fast intra-operative monitoring in order to avoid early or late neurological sequels, including the ones arising from surgical manipulation. The wide applicability of the ORD comes from its computational simplicity, being usually based on the calculation of parameters derived from the Fourier Transform of EEG epochs.

When a very low signal-to-noise ratio is observed, which is the circumstance expected in hospital units due to the presence of electrical/electro-mechanic devices that generate electrical/electromagnetic interference, the use of more than one derivation, in a multivariate ORD approach, may improve the probability of detection without increasing in the exam duration. For this purpose, both scalp regions and frequencies more responsive should be employed in the objective detection. Moreover, in order to obtain faster response detection, the most higher stimulation frequency that does not result in decrease in the detection rates should be used.

For the right posterior tibial nerve SEP, presented as an illustration in this review, the maximum response frequency range is within the high beta and low gamma band (20-60 Hz); the best regions for SEP recording includes the central and parietal leads at the midline and parasagital line ipsilateral to the stimulated limb ([Cz], [C4] [Pz] and [P4]). The stimulation frequency of 9 Hz, instead of the often employed 5 Hz, can be used without diminishes the probability of detection. Hence, once the application of MORD produces an increase in the detection percentages compared to the MSC for the same M-value, it can, on the other hand, be employed to reduce the exam duration (M), whereas the detection probability is maintained.

Analogue results are expected for SEP obtained for the left tibial nerve and even for upper limbs, since the anatomical pathways follow similar routes, including decussation and somatotopic mapping. However, it should be effectively measured.

This review presented the theoretical background of ORD and MORD techniques applied to the Evoked Potential field. The historical aspects together with the included examples may be useful to many researches, since they encompass applications ranging from elementary goals up to the state of art in biosignal detection.

8. Future directions

Based on the prominent results found by using multivariate objective response detection techniques, it would be useful to investigate it for a number of derivations higher than $N = 2$. The MCSM critical value does not vary with N, as stated on expression (26) (Felix and Miranda de Sá, 2003). Thus, augmenting the number of derivations would imply increasing the detection rate. However, it did not occur in practical applications (Melges, 2009, Felix *et al.*, 2007). This could be explained by the fact that the background activities are correlated and hence there would be no improvement by continuously adding new derivations. However, this hypothesis of correlated activities should be verified for different kinds of evoked potentials. Additionally, it would be worth to identify the optimal number of

derivations to be employed for both MC and MCSM estimation for each kind of stimulation, since the presence of a massive number of leads is undesirable for clinical and surgical monitoring purposes. Moreover, the exponential forgetting, suggested by Tierra-Criollo *et al.* (1998), should be applied for multivariate ORD in order to increase the rapidness of response detection. Finally, both ORD and MORD techniques should be incorporated in the EP analysis software to have their efficacy evaluated for diagnosis and neuro-monitoring.

9. Abbreviations

EEG – Electroencephalogram; EP – Evoked Potential; AEP – auditory EP; SEP – somatosensory EP; VEP – Visual EP; ORD – Objective Response Detection; MORD – Multivariate ORD.

10. Acknowledgements

To the Brazilian research and education agencies, the Rio de Janeiro State Research Council (FAPERJ), the National Council for Scientific and Technological Development (CNPq - Ministry of Science and Technology) and CAPES (Ministry of Education) for the financial support. We also acknowledge the Military Police Central Hospital of Rio de Janeiro for providing infrastructure support.

11. References

Angel, A, Linkens, DA, Ting, CH. 1999. Estimation of latency changes and relative amplitudes in somatosensory evoked potentials using wavelets and regression, *Comput Biomed Res*, Vol. 32, No. 3, Jun, pp. 209-251.

Beagley, HA, Sayers, BMcA, Ross, AJ. 1979. Fully objective ERA by phase spectral analysis, *Acta otolaryngol*, Vol. 87, No. 3, Jan, pp. 270-278.

Bendat, JS, Piersol, AG. 2000. *Random Data Analysis and Measurement Procedures* (3 ed), New York, Wiley-Interscience.

Bose, B, Sestokas, AK, Schwartz, DM. 2004. Neuropsychological monitoring of spinal cord function during instrumented anterior cervical fusion, *Spine J*, Vol. 4, No. 2, Mar/Apr, pp. 202-207.

Cagy, M, Infantosi, AFC, Gemal, AE. 2000. Monitoring depth of anaesthesia by frequency-domain statistical techniques, *Braz J Biomed Eng*, Vol. 16, No. 2, pp. 95-107.

Cagy, M, Infantosi, AFC. 2002. Unconsciousness indication using time-domain parameters extracted from mid-latency auditory evoked potentials, *J Clin Monit Comput*, Vol. 17, No.6, pp. 362-366.

Cagy, M., 2003, Monitorização do plano anestésico usando o potencial evocado auditivo de média latência: técnicas no domínio do tempo e coerência espectral. D.Sc. Thesis., COPPE/UFRJ, Rio de Janeiro, Rio de Janeiro, Brazil.

Cagy, M, Infantosi, AFC. 2007. Objective response detection technique in frequency-domain for reflecting changes in MLAEP, Medl Eng Phy, Vol 29, No 8, Oct, pp. 910-917.

Campos, DV, Infantosi, AFC, Lazarev, VV. 2006. Aplicação do Teste F spectral na detecção de respostas fotorecrutantes no eletroencefalograma multicanal de pacientes epilépticos, *Anais do XX Congresso Brasileiro de Engenharia Biomédica - CBEB2006* (CDROM), pp. 318-321, São Pedro, São Paulo, Brazil, Oct 2006.

Cruccu, G, Aminoff, MJ, Curio, G, Guerit, JM, Kakigi, R, Mauguière, F, Rossini, PM, Treede, R-D, Garcia-Larrea, L. 2008. Recommendations for the clinical use of somatosensory-evoked potentials, *Clin Neurophysiol*, Vol. 119, pp. 1705–1719.

Cruse R, Klem G, Lesser RP, Leuders H. 1982. Paradoxical lateralization of cortical potentials evoked by stimulation of posterior tibial nerve, *Arch Neurol*, Vol. 39, pp. 222-225.

Dobie, RA, Wilson, MJ. 1989. Analysis of auditory evoked potentials by Magnitude-Squared Coherence. *Ear Hear*, Vol. 10, No. 1, Fev, pp. 2-13.

Dobie, RA, Wilson, MJ. 1990. Optimal ('Wiener') digital filtering of auditory evoked potentials: use of coherence estimates. *Electroencephalogr Clin Neurophysiol*, Vol. 77, No. 3, May/Jun, pp. 205-213.

Dobie, RA, Wilson, MJ. 1993. Objective response detection in the frequency domain, *Electroencephalogr Clin Neurophysiol*, Vol. 88, No. 6, Nov/Dec, pp. 516-524.

Dobie, RA, Wilson, MJ. 1994a. Objective detection of 40Hz auditory evoked potentials: phase coherence vs. magnitude-squared coherence, *Electroencephalogr Clin Neurophysiol*, Vol. 92, No. 5, Set, pp. 405-413.

Dobie, RA, Wilson, MJ. 1994b. Phase weighting: a method to improve objective detection of steady-state evoked potentials, *Hear Res*, Vol. 79, No. 1-2, Set, pp. 94-98.

Dobie, RA, Wilson, M J. 1995. Objective versus human observer detection of 40 Hz auditory-evoked potentials, *J Acoustic Soc Am*, Vol. 97, No. 5, Mai, pp. 3042-3050.

Dobie, RA, Wilson, MJ. 1996. A comparison t test, F test and coherence methods of detecting steady-state auditory-evoked potentials, distortion product otoacoustic emissions, or other sinusoids, *J Acoustic Soc Am*, Vol. 100, No. 4, Out, pp. 2236-2246.

Dong, CC, MacDonald, DB, Janusz, MT. 2002. Intraoperative spinal cord monitoring during descending thoracic and thoracoabdominal aneurysm surgery, *Ann Thorac Surg*, Vol. 74, pp. S1873-S1876.

Faberowski, LW, Black S., Trankina, M.F., Polland, RJ, Clarck, RK, Mahla, ME. 1999. Somatosensory-evoked potentials during aortic coarctation repair, *J Cardiothorac Vasc Anesth*, Vol. 13, No. 5, Out, pp. 538-543.

Farina Jr, PD, Melges, DB, Miranda de Sá, AMFL, Infantosi, AFC. 2010. Técnica de detecção objetiva de resposta baseada na distribuição de Rice, *Anais do XXII Congresso Brasileiro de Engenharia Biomédica - CBEB2010*, [ISSN: 2179-3220], pp. 915-918, Tiradentes, Minas Gerais, Brazil, Nov 2010.

Felix, LB, Miranda de Sá, AMFL, Infantosi, AFC, Yehia, HC. 2007. Multivariate objective response detectors (MORD): statistical tools for multichannel EEG analysis, Ann Biomed Eng, Vol. 35, No. 3, Mar, pp. 443-452.

Ferreira, DD, Miranda de Sá, AMFL. 2005. Análise do EEG durante estimulação sensorial baseada nas funções de coerência simples, múltipla e parcial, *Braz J Biomed Eng*, Vol. 21, No. 1, pp. 5-14.

Florence, G, Guérit, J-M, Gueguen, B. 2004. Electroencephalography and somatosensory evoked potentials to prevent cerebral ischaemia in the operating room, Clin Neurophysiol, Vol. 34, No. 1, Fev, pp. 17-32.

Galambos, R, Makeig, S, Stapells, DR. 1984. The phase aggregation of steady state (40Hz) event related potentials: its use in estimating hearing thresholds. *XVII International Congress of Audiology*, Santa Barbara, California, Aug 1984.

Ghariani, S, Spaey, J, Liard, L, Verhelst, R., El Khoury, G, Noirhomme, P, D'udekem, Y., Matta, A, Dion, R, Guérit, J-M. 1998. Sensibilité, specificité et impact sur la stratégie

chirurgicale du neuromonitorage peropératoire par potentiels évoqués somesthésiques em chirurgie vasculaire pratiquée avec arrêt circulatoire sous hypothermie profonde, *Neurohpisiol Clin*, Vol. 28, No. 4, Set, pp. 335-342.

Ghariani, S, Liard, L, Spacy, J, Noirhomme, PH, Khoury, GAE, Tourtchaninoff, M, Dion, RA, Guérit, J-M. 1999. Retrospective study if somatosensory evoked potential monitoring in deep hypothermic circulatory arrest, *Ann Thorac Surg*, Vol. 67, No. 6, Jun, pp. 1915-1918.

Ghariani, S, Matta, A, Dion, R, Guérit, J-M. 2000. Intra- and postoperative factors determining neurological complications after surgery under deep hypothermic circulatory arrest: a retrospective somatosensory evoked potential study, *Clin Neurophysiol*, Vol. 111, No. 6, Jun, pp. 1082-1094.

Gemal, AE. 1999. Changes in the auditory middle latency response to propofol infusions. Ph.D. Thesis, University of Bristol, Bristol, England.

Giugno, K M, Maia, TR, Kunrath, CL, Bizzi, JJ. 2003. Tratamento da hipertensão intracraniana, *Jornal de Pediatria*, Vol. 79, No. 4, Jul/Aug, pp. 287-296.

Greenblatt, E, Zapulla, RA, Kaye, S, Friedman, J. 1985. Response threshold determination of the brain stem auditory evoked response: a comparison of the phase versus magnitude derived from the Fast Fourier Transform, *Int J Audiol*, Vol. 24, No. 4, Jan, pp. 288-296.

Guérit, J-M. 1999. Medical technology assessment EEG and evoked potentials in the intensive care unit, *Clin Neurophysiol*, Vol. 29, No. 4, Sep, pp. 301-317.

Guérit, J-M, Dion, RA. 2002. State-of-the art of neuromonitoring for prevention of immediate and delayed paraplegia in thoracic and thoracoabdominal aorta surgery, *Ann Thorac Surg*, No. 74, pp. S1867-S1869.

Gundanna, M, Eskenasi, M, Bendo, J, Spivak, J, Moskovich, R. 2003. Somatosensory evoked potential monitoring of lumbar pedicle screw placement for in situ posterior spinal fusion, *Spine J*, Vol. 3, No. 5, Sep/Oct, pp. 370-376.

Hotelling, H. 1931. The generalization of Student's ratio, *Ann Math Stat*, Vol. 2, pp. 360-378.

Infantosi, AFC, Cagy, M, Zaeyen, EJB. 2004. Aplicação da Magnitude Quadrática da Coerência ao MLAEP com estimulação a baixos níveis de pressão sonora. *IFMBE Proceedings - III Congreso Latinoamericano de Ingeniería Biomédica – CLAIB2004 (CDROM)*, Vol. 5, pp. 1111-1114, João Pessoa, Paraíba, Brazil, 2004.

Infantosi, AFC, Melges, DB, Miranda de Sá, AMFL, Cagy, M. 2005. Uni- and multi-variate coherence-based detection applied to EEG during somatosensory stimulation, *IFMBE Proceedings - 3rd. European Medical & Biological Engineering Conference - EMBEC'2005 (CDROM)*, Vol. 11, pp. 1-4 (578F.pdf), Prague, Czech Republic, 2005.

Infantosi, AFC, Melges, DB, Tierra-Criollo, CJ. 2006. Use of magnitude-squared coherence to identify the maximum driving response band of the somatosensory evoked potential, *Braz J Med Biol Res*, Vol. 39, pp. 1593-1603.

Infantosi, AFC, Miranda de Sá, AMFL. 2006. A coherence-based technique for separating phase-locked from non-phase-locked power spectrum estimates during intermittent stimulation, *J Neurosci Methods*, Vol. 156, No. 1-2, Set, pp. 267-274.

Hoffmann, MB, Seufert, PS, Bach, M. 2004. Simulated nystagmus suppresses pattern-reversal but not pattern-onset visual evoked potentials, *Clin Neurophysiol*, Vol. 115, No. 11, Nov, pp. 2659-2665.

Holopigian, K, Shuwairi, SM, Greenstein, VC, Winn, BJ, Zhang, X., Carr, RE, Hood, DC. 2005. Multifocal visualevokedpotentials to cone specific stimuli in patients with retinitis pigmentosa, Vision Research, Vol. 45, No. 25-26, Nov, pp. 3244-3252

Jancic-Stefanovic, JB, Stefanovic, DM, Obradovic, D, Cetkovic, MV. 2003. Visual-evokedpotentials as additional diagnostic procedure in migraine headaches in childhood and adolescence, *International Congress Series*, Vol. 1240, Oct, pp. 1395-1398.

Jones, SC, Fernau, R, Woeltjen, BL. 2004. Use of somatosensory evoked potentials to detect peripheral ischemia and potential injury resulting from positioning of the surgical patient: case reports and discussion, *Spine J*, Vol. 4, No. 4, May/Jun, pp. 360-362.

Kato, T, Okumura, A, Hayakawa, F, Kuno, K, Watanabe, K. 2005. The evolutionary change of flash visual evoked potentials in preterm infants with periventricular leukomalacia, *Clin Neurophysiol*, Vol. 116, No. 3, Mar, pp. 690-695.

Keyhani, K, Miller III, CC, Estrera, AL, Wegryn, T, Sheinbaum, R, Safi, HJ. 2009. Analysis of motor and somatosensory evoked potentials during thoracic and thoracoabdominal aortic aneurysm repair, *J Vasc Surg* 49 p. 36-41.

Klein, A, Sauer, T, Jedynak, A, Skrandies, W. 2006. Conventional and Wavelet Coherence applied to sensory-evoked electrical brain activity, *IEEE Trans Biomed Eng*, Vol. 53, No. 2, Fev, pp. 266-272.

Krishnan, GP, Vohs, JL, Hetrick, WP, Carroll, CA, Shekhar,A, Bockbrader, MA, O'Donnell, BF. 2005. Steady state visual evoked potential abnormalities in schizophrenia, *Clin Neurophysiol*, Vol. 116, No. 3, Mar, pp. 614-624.

Liavas, AP, Moustakides, GV, Henning, G, Psarakis, EZ, Husar, P. 1998. A periodogram-based method for the detection of steady-state visually evoked potentials, *IEEE Trans Biomed Eng*, Vol. 45, No. 2, Fev, pp. 242-248.

Linden, RD, Zappula, R, Shields, CB. 1997. Intraoperative evoked potential monitoring. In: *Evoked Potentials in Clinical Medicine*, Chiappa, KH, pp. 601-638, Raven Press, New York, USA.

Liu, H, Di Giorgio, AM, Williams, ES, Evans, W, Russell, MJ. 2010. Protocol for electrophysiological monitoring of carotid endarterectomies, *J Biomed Res.*, Vol. 24, pp. 460-466.

Logi, F, Fisher, C, Murri, L, Mauguière, F. 2003. The prognostic value of evoked responses from primary somatosensory and auditory in comatose patients, *Clin Neurophysiol*, Vol. 114, No. 9, Set, pp. 1615-1627.

Lopes da Silva, F. 1999. Event-Related Potentials: Methodology and Quantification. In: *Electroencephalography - Basic Principles, Clinical Applications, and Related Fields*, Niedermeyer, E, Lopes da Silva, FH (eds), 4 ed., chapter 52, Baltimore, USA, Williams &Wilkins.

Mardia, KV. 1972. *Statistics of Directional Data*. 1 ed. London, Academic Press.

Martin, CJ, Sinson, G, Patterson, T, Zager, EL, Stecker MM. 2002. Sensitivity of scalp EEG, cortical EEG, and somatosensory evoked responses during surgery for intracranial aneurysms, *Surg Neurol*, Vol. 58, No. 5, Nov, pp. 317-321.

Melges, DB, 2005, A Virtual Instrument for Somatosensory stimulation response monitoring. M.Sc. Dissertation, COPPE/UFRJ, Rio de Janeiro, Rio de Janeiro, Brazil. (Available at: http://www.dominiopublico.gov.br/)

Melges, DB, Infantosi, A FC, Cagy, M, Miranda de Sá, AMFL. 2005. The Magnitude-Squared Coherence in the Detection of Stimulation/No-Stimulation Transitions, *IFMBE Proceedings - 13th Nordic Baltic Conference - Biomedical Engineering and Medical Physics*, [ISSN 1680-0737], Vol. 9, pp. 58-59, Umea, Suécia, 2005.

Melges, DB, Miranda de Sá, AMFL, Infantosi, AFC. 2006a. Using Component Synchrony Measure for somatosensory evoked potential detection, *Proceedings of the 28 th Annual International Conference IEEE - Engineering in Medicine and Biology Society– EMBC' 2006* [ISSN: 1557-170X], pp. 4572-4575, New York, USA, Aug/Sept 2006.

Melges, DB, Miranda de Sá, AMFL, Infantosi, AFC. 2006b. Técnicas multivariadas de detecção objetiva aplicadas ao EEG durante estimulação somato-sensitiva, *Anais do XX Congresso Brasileiro de Engenharia Biomédica - CBEB2006 (CDROM)*, pp. 338-341, São Pedro, São Paulo, Brazil, Oct 2006.

Melges, DB, Infantosi, AFC, Miranda de Sá, AMFL. 2008a. Topographic distribution of the tibial somatosensory evoked potential using coherence, *Braz J Med Biol Res*, Vol. 41, No. 12, Dec, pp. 1059-1066.

Melges, DB, Infantosi, AFC, Miranda de Sá, AMFL. 2008b. Detecção da resposta somato-sensitiva: coerência simples (derivações bipolares) vs múltipla (unipolares), *Anais do XXI Congresso Brasileiro de Engenharia Biomédica - CBEB' 2008* [ISBN: 978-85-60064-13-7], Vol. 1, pp. 1671-1674, Salvador, Bahia, Brazil, Nov 2008.

Melges, DB, 2009, Uni and multivariate frequency-domain objective response detection techniques application to the EEG during somatosensory stimulation. D.Sc. Thesis, COPPE/UFRJ, Rio de Janeiro, Rio de Janeiro, Brazil. (Available at: http://www.dominiopublico.gov.br/)

Melges, DB, Miranda de Sá, AMFL, Infantosi, AFC. 2010. Multiple Coherence vs Multiple Component Synchrony Measure for somatosensory evoked response detection, *Proceedings of the 32nd Annual International Conference of the IEEE Engineering in Medicine and Biology Society – EMBC' 2010* [ISSN: 1557-170X], pp. 1662-1665, Buenos Aires, Argentina, Aug/Sep 2010.

Melges, DB, Infantosi, AFC, Miranda de Sá, AMFL. 2011a. Using Objective Response Detection techniques for detecting the tibial somatosensory evoked response with different stimulation rates, *J Neurosci Methods*, Vol. 195, pp.255-260.

Melges, DB, Miranda de Sá, AMFL, Infantosi, AFC. 2011b. Tibial nerve somatosensory evoked response detection using uni and multivariate coherence. *Biomed Signal Process Control* (*in press*).

Miranda de Sá, AMFL, Simpson, DM, Infantosi, AFC. 1994. Estudo da função de coerência aplicada a sinais EEG, *Braz J Biomed Eng*, Vol. 10, No. 2, pp. 39-55.

Miranda de Sá, AMFL. 2000. Desenvolvimento de técnicas para o estudo da coerência no EEG durante foto-estimulação intermitente. D.Sc. Thesis, COPPE/UFRJ, Rio de Janeiro, Rio de Janeiro, Brazil.

Miranda de Sá, AMFL, Infantosi, AFC, Simpson, DM. 2001. A statistical technique for measuring synchronism between cortical regions in the EEG during rhythmic stimulation, *IEEE Trans Biomed Eng*, Vol. 48, No. 10, Oct, pp. 1211-1215.

Miranda de Sá, AMFL, Felix, LB. 2002. Improving the detection of evoked responses to periodic stimulation by using multiple coherence – application during photic stimulation, *Med Eng Phys*, Vol. 24, No. 4, May, pp. 245-252.

Miranda de Sá, AMFL, Infantosi, AFC. 2002. A coherence-based technique for evaluating the degree of synchronism in the EEG during sensory stimulation, *Braz J Biomed Eng*, Vol. 18, No. 1, Jan/Apr, pp. 39-49.

Miranda de Sá, AMFL, Infantosi, AFC, Simpson, DM. 2002. Coherence between one random and one periodic signal for measuring the strength of responses in the EEG during sensory stimulation, *Med Biol Eng Comput,* Vol. 40, pp. 99-104.

Miranda de Sá, AMFL, Felix, LB. 2003. Multi-channel evoked response detection using only phase information, *J Neurosci Methods*, Vol. 129, No. 1, Oct, pp. 1-10.

Miranda de Sá, AMFL. 2004. A note on the sampling distribution of coherence estimate for the detection of periodic signals, *IEEE Signal Process Lett*, Vol. 11, No. 3, Mar, pp. 323-325.

Miranda de Sá, AMFL, Felix, LB, Infantosi, AFC. 2004. A matrix-based algorithm for estimating multiple coherence of periodic signal and its application to the multichannel EEG during sensory stimulation, *IEEE Trans Biomed Eng*, Vol. 51, No. 7, Jul, pp. 1140-1146.

Miranda de Sá, AMFL, Cagy, M, Melges, DB, Infantosi, AFC. 2005. Multivariate spectral analysis applied to the EEG during rhythmic stimulation – a coherence-based approach, *IFMBE Proceedings - 13th Nordic Baltic Conference - Biomedical Engineering and Medical Physics* [ISSN 1680-0737], Vol. 9, pp. 60-61, Umea, Suécia, Jun 2005.

Miranda de Sá, AMFL. 2006a, A note on the coherence-based signal-to-noise ratio estimation in systems with periodic inputs, *J Franklin Institute*, Vol. 343, No. 7, Nov, pp. 688-698.

Miranda de Sá, AMFL. 2006b. Evaluating spectral relationships between signals by removing the contribution of a common, periodic source – a partial coherence-based approach, *Inter J Biomed Sci*, Vol. 1, No. 1, pp. 15-18.

Miranda de Sá, AMFL, Cagy, M, Lazarev, VV, Infantosi, AFC. 2006. Spectral F-test power evaluation in the EEG during intermittent photic stimulation, *Arq Neuropsiquiatr*, Vol. 64, n. 2-A, Jun, pp. 228-232.

Miranda de Sá, AMFL, Infantosi, AFC. 2007. Evaluating the relationship of non-phase locked activities in the electroencephalogram during intermittent stimulation: a partial coherence-based approach, *Med Biol Eng Comput*, Vol. 45, pp. 635-642.

Miranda de Sá, AMFL, Infantosi, AFC, Melges, DB. 2008. A multiple coherence-based detector for evoked responses in the EEG during sensory stimulation, *Proceedings of the 30th Annual International Conference of the IEEE Engineering in Medicine and Biology Society– EMBC' 2008* [ISSN: 1557-170X], p. 3516-3519, Vancouver, Canada, Aug 2008.

Miranda de Sá, AMFL, Ferreira, DD, Dias, EW, Mendes, EMAM, Felix, LB. 2009. Coherence estimate between a random and a periodic signal: bias, variance, analytical critical values and normalizing transforms, *J Franklin Institute*, Vol. 346, pp. 841-853.

Nayak, A, Roy, RJ. 1998. Anesthesia control using midlatency auditory evoked potentials, *IEEE Trans Biomed Eng*, Vol. 45, No. 4, Apr, pp. 409-421.

Nemoto, N, Mori, H, Kiyosawa, M, Wang, WF, Mochizuki, M, Momose, K. 2002. Visual Evoked Potentials Elicited by Pseudorandom Stimulation from Patients with Macular Degeneration, *Japanese Journal of Ophthalmology*, Vol. 46, No. 1, pp. 108-113.

Nuwer, MR, Dawson, EG, Carlson, LG, Kanim, Le, A, Sherman, JE. 1995. Somatosensory evoked potential spinal cord monitoring reduces neurologic deficits after scoliosis

surgery: results of a large multicenter survey, *Electroencephalogr Clin Neurophysiol*, Vol. 96, No. 1, Jan, pp. 6-11.

Pacheco, EA. 2003. Determinação da banda de máxima resposta do potencial evocado auditivo de curta latência por meio da magnitude quadrática da coerência. M.Sc. Dissertation, COPPE/UFRJ, Rio de Janeiro, Rio de Janeiro, Brazil.

Pacheco, EA, Infantosi, AFC. 2005. Determinação das Bandas de Máxima Resposta Espectral do Potencial Evocado Auditivo de Tronco Cerebral Utilizando a Magnitude Quadrática da Coerência, *Braz J Biomed Eng*, Vol. 21, No. 3, pp. 105-113.

Parisi, V, Manni, G, Centofanti, M, Gandolfi, SA, Olzi, D, Bucci, MG. 2001. Correlation between optical coherence tomography, pattern electroretinogram, and visual evoked potentials in open-angle glaucoma patients, *Ophthalmology*, Vol. 108, No. 5, May, pp. 905-912.

Picton, TW, Vajsar, J, Rodriguez, R, Campbell, KB. 1987. Reliability estimates for steady-state evoked potentials, *Electroencephalogr Clin Neurophysiol/Evoked Potentials Section*, Vol. 68, No. 2, Mar, pp. 119-131.

Ramos, EG, Zaeyen, EJB, Simpson, DM, Infantosi, AFC. 2000. Detecção da resposta auditiva no EEG de crianças utilizando técnicas no domínio da freqüência, *Braz J Biomed Eng*, Vol. 16, No. 3, Sep/Dec, pp. 127-137.

Simpson, DM, Tierra-Criollo, CJ, Leite, RT, Zaeyen, EJB, Infantosi, AFC. 2000. Objective response detection in an electroencephalogram during somatosensory stimulation, *Ann Biomed Eng*, Vol. 28, No. 6, Jun, pp. 691-698.

Schulte-Körne, G, Bartling, J, Deimel, W, Remschmidt, H. 2004. Visual evoked potentials elicited by coherently moving dots in dyslexic children, Clin Neurophysiol, Vol. 115, No. 3, Mar, pp. 207-120.

Stapells, DR, Makeig, S, Galambos, R. 1987. Auditory steady state responses: threshold prediction using phase coherence, *Electroencephalogr Clin Neurophysiol*, Vol. 67, No. 3, Sep, pp. 260-270.

Thakor, NV, Kong, X, Handley, DF. 1995. Nonlinear changes in brain's response in the event of injury as detected by adaptive coherence estimation of evoked potentials, *IEEE Trans Biomed Eng*, Vol. 42, No. 1, Jan, pp. 42-51.

Tierra-Criollo, CJ, Zaeyen, EJB, Simpson, DM, Infantosi, AFC. 1998. Detecção da resposta à estimulação somato-sensitiva no EEG utilizando a Magnitude Quadrada da Coerência Ponderada, *Anais do IV Fórum Nacional de Ciência e Tecnologia em Saúde*, pp. 441-442, Curitiba, Paraná, Brazil, Oct 1998.

Tierra-Criollo, CJ. 2001. Monitorização objetiva da resposta à estimulação somato-sensitiva utilizando parâmetros espectrais. D.Sc. Thesis, COPPE/UFRJ, Rio de Janeiro, Rio de Janeiro, Brazil.

Trisciuzzi, MTS, Riccardi, R, Piccardi, M, Iarossi, G, Buzzonetti, L, Dickmann, A, Colosimo, C, Ruggiero, A, Di Rocco, C, Falsini, B. 2004. A fast visualevokedpotential method for functional assessment and follow-up of childhood optic gliomas, Clin Neurophysiol, Vol. 115, No. 1, Jan, pp. 217-226

Van Dongen, EP, Schepens, MA, Morshuis, WJ, Ter Beek, HT, Aarts, LP, De Boer, A, Boezeman, EH. 2001. Thoracic and thoracoabdominal aortic aneurysm repair: Use of evoked potential monitoring in 118 patients, J Vasc Surg, Vol. 34, No. 6, Dec, pp. 1035-1040.

Victor, JD, Mast, J. 1991. A new statistic for steady-state evoked potentials, Electroencephalogr Clin Neurophysiol, Vol. 78, No. 5, May, pp. 378-388.

Xu, S, Meyer, D, Yoser, S, Mathews, D, Elfervig, JL. 2001.Pattern visual evoked potential in the diagnosis of functional visual loss, *Ophthalmology*, Vol. 108, No. 1, Jan, pp. 76-80.

Zaeyen, EJB. 2005. Aplicação da Coerência ao eletroencefalograma para investigar características do Potencial Evocado Auditivo de Média Latência. M.Sc. Dissertation, COPPE/UFRJ, Rio de Janeiro, Rio de Janeiro, Brazil. (Available at: http://www.dominiopublico.gov.br/)

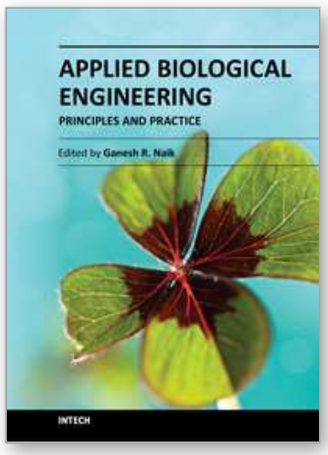

Applied Biological Engineering - Principles and Practice
Edited by Dr. Ganesh R. Naik

ISBN 978-953-51-0412-4
Hard cover, 662 pages
Publisher InTech
Published online 23, March, 2012
Published in print edition March, 2012

Biological engineering is a field of engineering in which the emphasis is on life and life-sustaining systems. Biological engineering is an emerging discipline that encompasses engineering theory and practice connected to and derived from the science of biology. The most important trend in biological engineering is the dynamic range of scales at which biotechnology is now able to integrate with biological processes. An explosion in micro/nanoscale technology is allowing the manufacture of nanoparticles for drug delivery into cells, miniaturized implantable microsensors for medical diagnostics, and micro-engineered robots for on-board tissue repairs. This book aims to provide an updated overview of the recent developments in biological engineering from diverse aspects and various applications in clinical and experimental research.

InTech Europe
University Campus STeP Ri
Slavka Krautzeka 83/A
51000 Rijeka, Croatia
Phone: +385 (51) 770 447
Fax: +385 (51) 686 166
www.intechopen.com

InTech China
Unit 405, Office Block, Hotel Equatorial Shanghai
No.65, Yan An Road (West), Shanghai, 200040, China
中国上海市延安西路65号上海国际贵都大饭店办公楼405单元
Phone: +86-21-62489820
Fax: +86-21-62489821

IntechOpen